Scientific Reports

https://doi.org/10.1038/s41598-026-50028-w

Article in Press

Circulating CD38^{+} regulatory T cells are decreased in bone fracture non-union with chronic subclinical infection

Received: 15 December 2025

Accepted: 17 April 2026

Published online: 27 April 2026

Cite this article as: Fehrenbach P., Siverino C., Trenkwalder K. *et al.* Circulating CD38^{+} regulatory T cells are decreased in bone fracture non-union with chronic subclinical infection. *Sci Rep* (2026). https://doi.org/10.1038/s41598-026-50028-w

Pia Fehrenbach, Claudia Siverino, Katharina Trenkwalder, Sandra Erichsen, Simon Hackl, Ferdinand Weisemann, Gowrishankar Muthukrishnan, Martijn Riool, Cezmi A. Akdis, Juan J. Garcia-Vallejo, Sebastian A. J. Zaat, Esther C. Jong & Thomas Fintan Moriarty

Circulating CD38^{+} regulatory T cells are decreased in bone fracture non-union with chronic subclinical infection

Pia Fehrenbach[1,2], Claudia Siverino[1], Katharina Trenkwalder[3,4], Sandra Erichsen[3,4], Simon Hackl[5], Ferdinand Weisemann[5], Gowrishankar Muthukrishnan[6], Martijn Riool[7,8], Cezmi A. Akdis[9], Juan J. Garcia Vallejo[10], Sebastian A. J. Zaat[8], Esther C. de Jong[2], Thomas Fintan Moriarty[1,11*]

[1]AO Research Institute Davos, Davos, Switzerland, [2]Amsterdam AMC, Department of Experimental Immunology, Amsterdam institute for Immunology and Infectious Diseases, University of Amsterdam, Amsterdam, The Netherlands, [3]Institute for Biomechanics, Paracelsus Medical University Salzburg, Salzburg, Austria, [4]Institute for Biomechanics, BG Unfallklinik Murnau, Murnau, Germany, [5]Department of Trauma Surgery, BG Unfallklinik Murnau, Murnau, Germany, [6]Center for Musculoskeletal Research, Department of Orthopaedics, University of Rochester Medical Center, Rochester, NY, United States, [7]University Hospital Regensburg, Department of Trauma Surgery, Regensburg, Germany, [8]Amsterdam UMC, Department of Medical Microbiology and Infection Prevention, Amsterdam institute for Immunology and Infectious Diseases, University of Amsterdam, Amsterdam, The Netherlands, [9]Swiss Institute of Allergy and Asthma Research (SIAF), Davos, Switzerland, [10]Amsterdam UMC, Department of Experimental Immunology, Amsterdam UMC, Vrije Universiteit, Amsterdam, The Netherlands, [11]Center for Musculoskeletal Infection, University Hospital Basel, Basel, Switzerland

*Corresponding author: fintan.moriarty@aofoundation.org

Abstract

Fracture non-union represents a complex clinical challenge resulting from an incompletely understood interplay between mechanical and biological factors. Infection frequently contributes to non-union but many cases are misdiagnosed due to lack of classical clinical symptoms. This study characterized peripheral blood mononuclear cells (PBMCs) from aseptic non-union (NU-AS, n=24) and fracture-related infected non-union (NU-FRI, n=20) and compared healed controls (H, n=18). High-dimensional mass cytometry (CyTOF) revealed significant elevations of regulatory T cells (Tregs; p=0.0028) and T helper 1 (Th1) cells (p=0.0073), and reduced expression of the activation marker CD38 in $CD4^+$ T cells (p=0.0016) and Tregs (p=0.0017) in NU compared to H. In a sub-group analysis between NU-AS and NU-FRI, monocyte and $CD38^+$ Treg cell counts provided excellent diagnostic potential, with the combination achieving a sensitivity of 100% and a specificity of 91.7%. These findings highlight an important role of the activation marker CD38 in diagnosing chronic subclinical infection which promises earlier identification of appropriate management of these patients.

Key words:

Non-union; Fracture healing; T regulatory cells; Treg; Fracture-related infection; CD38

Background

Every year, approximately 178 million bone fractures occur worldwide (1), primarily due to events such as motor vehicle accidents and falls. While most fractures heal successfully, up to 10% of long bone fractures may experience delayed healing or failure to heal, often referred to as non-union (NU) (2, 3). Clinically, NU is defined as failure of a fracture to heal without additional surgical intervention, independent of the duration of previous treatment (1, 4, 5). Patient-dependent risk factors for NU include advanced age, smoking, use of non-steroidal anti-inflammatory drugs, and comorbidities such as various genetic disorders, diabetes, and nutritional deficiencies (6). Patient-independent factors include the type, location and displacement of the fracture, the degree of soft tissue injury, extent of bone loss, quality of surgical treatment, and the presence of infection (6, 7). Moreover, mechanical instability is a well-recognized factor contributing to NU, disrupting normal healing by impairing callus formation and remodelling (8, 9).

The immune system plays an important role in fracture healing, as the initial injury triggers an early inflammatory response that recruits a range of immune cells to the injured tissue (10-12). The roles of innate immune cells, particularly neutrophils and macrophages, as early responders and key drivers of the initial inflammatory phase, are firmly established (13, 14). Macrophages subsequently release growth factors that support tissue repair (15, 16). In contrast, the role of adaptive immune cells is still emerging. T helper 1 (Th1) cells are critical in the early inflammatory phase, while T helper 2 (Th2) cells contribute to the later tissue repair phase (17, 18). Studies have shown that elevated Th1 and T helper 17 (Th17) cells may contribute to bone healing complications, as these cells are major sources of receptor activator of nuclear factor kappa-B ligand (RANKL), promoting osteoclast activity and bone resorption, especially under inflammatory conditions (18-20). Regulatory T cells (Tregs), in contrast, control inflammation in the early phase, facilitating proliferation and differentiation of osteogenic precursor cells (20, 21) and inhibiting osteoclast differentiation and bone resorption (21-23). These T cell subsets are driven by dendritic cells (DCs), which are critical for establishing immunological memory and tolerance(24), and therefore significantly contribute to bone healing (25). Early dysregulation between immune cells may negatively affect bone repair, with, for instance, patients with impaired mandibular fracture healing exhibit a higher preoperative ratio of $CD8^+$ T effector cells to $CD4^+$ Tregs (26). During infection, activated T cells typically upregulate CD38

expression, which enhances proinflammatory cytokine production, supports cell survival, and sustains metabolic activity (27-29). Following the clearance of infection, the CD38 expression typically returns back to baseline, however, in chronic infection, the CD38 remains elevated on PD-1^{+} exhausted CD8^{+} T cells (27, 30). Dysregulated B cell activity has also been implicated in healing complications, as patients with delayed bone healing displayed reduced regulatory B-cell activity and secretion of Interleukin 10 (IL-10) (31-33). Thus, the immune response is crucial for proper healing but is also implicated in healing complications.

Currently, a comprehensive understanding of how immune cells contribute to NU in human patients is lacking. The relative infrequency of NU, coupled with prolonged timeframes between initial fracture stabilization surgery and NU diagnosis, makes large-scale studies challenging. The goal of the present study was therefore to immunophenotype peripheral blood mononuclear cells (PBMCs) from patients with NU and compare the findings with control patients experiencing uneventful fracture healing. A primary objective was to identify differences in immune profiles of PBMCs between infected and aseptic NU, as this distinction substantially impacts treatment decisions but currently lacks adequate diagnostic modalities in patients without clinical symptoms of infection.

Results

In total, PBMCs from 18 healed (H) and 44 non-union (NU) patients underwent high-dimensional immune phenotyping by mass cytometry (CyTOF; 43-colour panel), examining innate and adaptive immune cell populations as well as activation and exhaustion markers. Thanks to group matching, no significant differences in age or gender distribution between groups were observed. However, NU patients had significantly higher BMI ($p<0.0001$), and a greater prevalence of diabetes ($p<0.0001$) compared to H patients, while H patients were more likely to be smokers ($p=0.018$).

T cell and granulocyte clusters differ between healed and non-union patients in peripheral blood

Initial analyses considered all NU patients as a single cohort. Uniform manifold approximation and projection (UMAP) representations of all PBMCs from H (Figure 1A) and NU patients (Figure 1B) illustrate the most abundant cell types in each group. UMAP plots indicated greater abundance of Tregs, granulocytes, and monocytes in NU compared to H patients.

Unsupervised clustering using PhenoGraph and edgeR identified 28 metaclusters, of which 7 showed significant differences in cell enrichment between H and NU patients (Figure 1C). A detailed heatmap with individual marker expression is available in Figure S1. Clusters enriched in NU patients included granulocytic/neutrophilic populations (C04, C15, C17), $CD4^+$ T cells (C18, C24), and $CD8^+$ T cells (C08) (Figure 1D). In contrast, γδ T cells (C13) were decreased in NU patients. UMAP visualizations of significantly altered clusters are shown for H (Figure 1E) and NU patients (Figure 1F). The heatmap visualization of cluster marker expression can be found in the supplements (Figure S1-3).

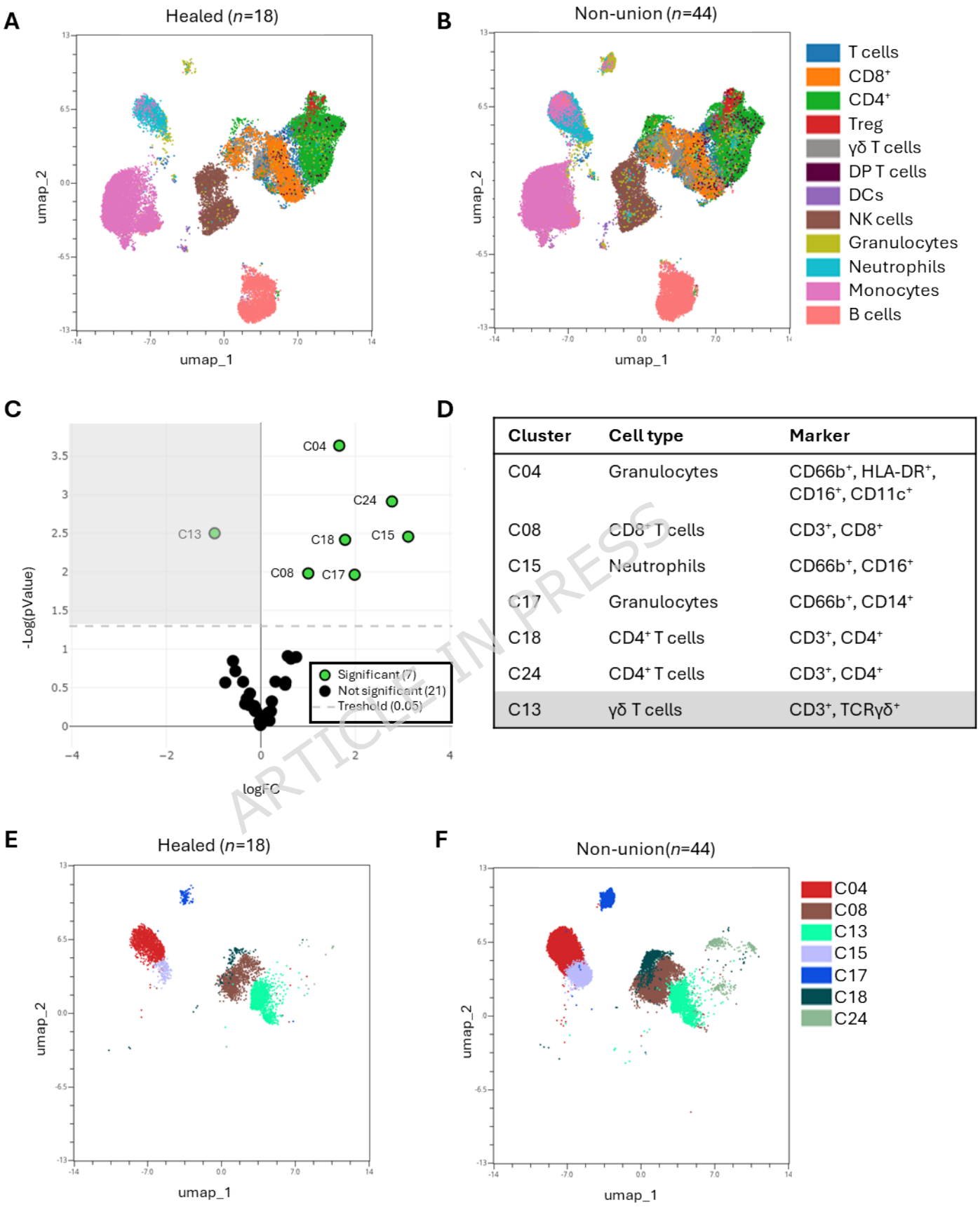

D

Cluster	Cell type	Marker
C04	Granulocytes	CD66b$^+$, HLA-DR$^+$, CD16$^+$, CD11c$^+$
C08	CD8$^+$ T cells	CD3$^+$, CD8$^+$
C15	Neutrophils	CD66b$^+$, CD16$^+$
C17	Granulocytes	CD66b$^+$, CD14$^+$
C18	CD4$^+$ T cells	CD3$^+$, CD4$^+$
C24	CD4$^+$ T cells	CD3$^+$, CD4$^+$
C13	γδ T cells	CD3$^+$, TCRγδ$^+$

Figure 1: Uniform manifold approximation and projection (UMAP) of PBMCs from all Healed and Non-union patients. UMAP representation of all cells from (A) H and (B) NU patients

coloured by lineage. (C) Volcano plot comparing proportions of 28 metaclusters (MC) between H and NU patients. The x-axis shows the difference in means of log2-transformed MC proportions; the y-axis shows the -log10-transformed Benjamini-Hochberg (BH)-adjusted p-value obtained using Welch's t-test. Green points above the horizontal line indicate significantly different clusters. Downregulated clusters are marked in grey. (D) Significantly different clusters with corresponding cell types and markers. UMAP representation of significantly different clusters in (E) H and (F) NU patients. Corresponding heatmaps are provided in Figure S1.

Increased CD4$^+$ T helper cell subsets in peripheral blood in non-union patients compared to healed patients

Because cluster analyses revealed significant differences in T cell populations, CD4$^+$ T helper cell subsets were further investigated at the individual patient level (Figure 2). NU patients had significantly higher proportions of Tregs (Figure 2A) and Th1 cells (Figure 2B) compared to H patients (p=0.0028 and p=0.0073, respectively). Conversely, T follicular helper (Tfh) cells (Figure 2D) were reduced in NU (p=0.0031). No significant differences were observed in Th2 cells (Figure 2C), γδ T cells (Figure S5I) or neutrophils (Figure S7B). Regarding activation markers, CD38$^+$ CD4$^+$ T cells (Figure 2E) and Tregs (Figure 2F) were significantly

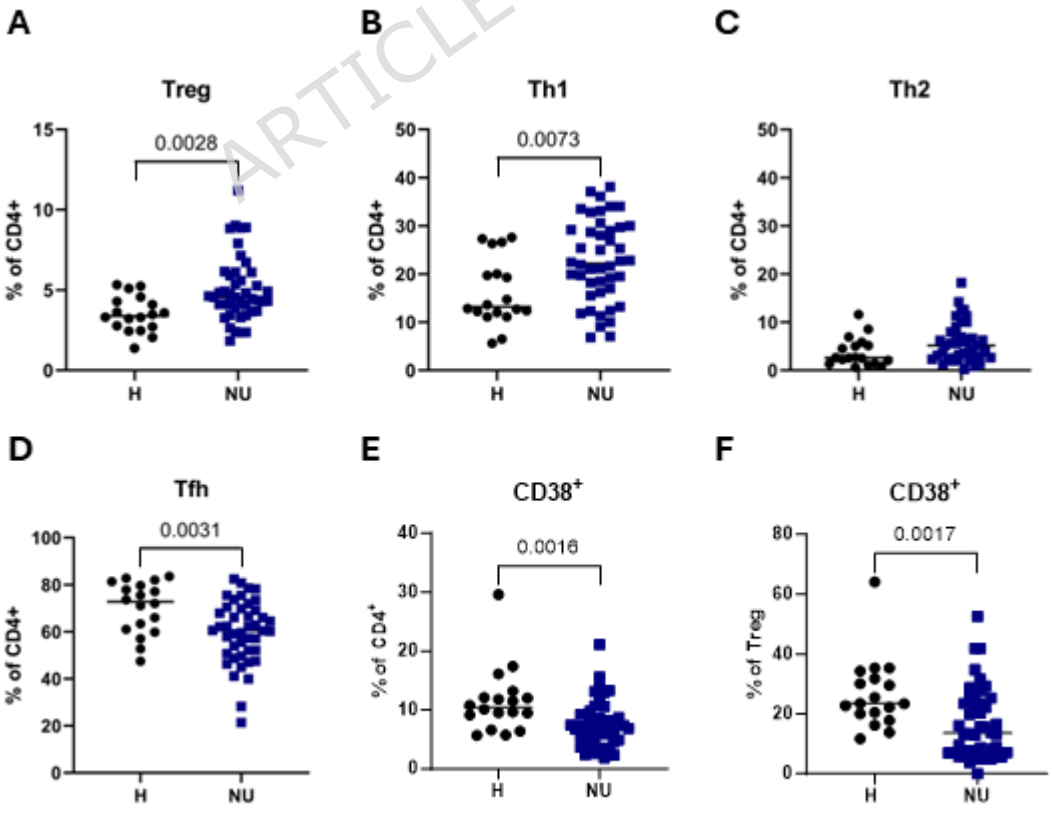

decreased in NU patients (p=0.0016 and p=0.0017, respectively). Additional immune cell analysis can be found in the supplements (Figure S4- S8).

Figure 2: CD4$^+$ T helper subsets and CD38$^+$ cells in Healed versus Non-union patients. (A) Tregs, (B) Th1 cells, (C) Th2 cells, (D) Tfh cells, (E) CD38$^+$ CD4$^+$ T cells, and (F) CD38$^+$ Tregs. Data shown are from individual patients (H: n=18; NU: n=44). Statistical analyses performed used Mann-Whitney or Welch's tests. Gating strategy: CD45$^+$CD66b$^-$, CD19$^-$CD20$^-$, CD3$^+$, CD4$^+$; Tregs: CCR4$^+$, CD45RA$^-$CD45RO$^+$, CD127^{low}CD25^{high}; Th1 cells: CD25$^-$, CXCR3$^+$CCR6$^-$; Th2 cells: CD25$^-$, CXCR3$^-$ CCR6$^-$; Tfh cells: CD25$^-$, CXCR3$^+$CCR6$^+$.

Fracture-related infection is associated with increased neutrophils and double positive T cells in peripheral blood

The NU cohort was subsequently stratified into aseptic NU (NU-AS) and fracture-related infected NU (NU-FRI) subgroups to examine how infection affects the systemic immune responses in NU. UMAP representation of all PBMCs from NU-AS (Figure 3A) and NU-FRI (Figure 3B) patients showed no visually apparent differences between the groups. However, clustering analysis identified 2 metaclusters significantly elevated in NU-FRI compared to NU-AS (Figure 3C): one cluster of neutrophils (C15) and a distinct double-positive (DP: CD4$^+$CD8$^+$) T cell cluster (C24; Figure 3D). UMAP representations of these significantly changed clusters are shown for NU-AS (Figure 3E) and NU-FRI patients (Figure 3F).

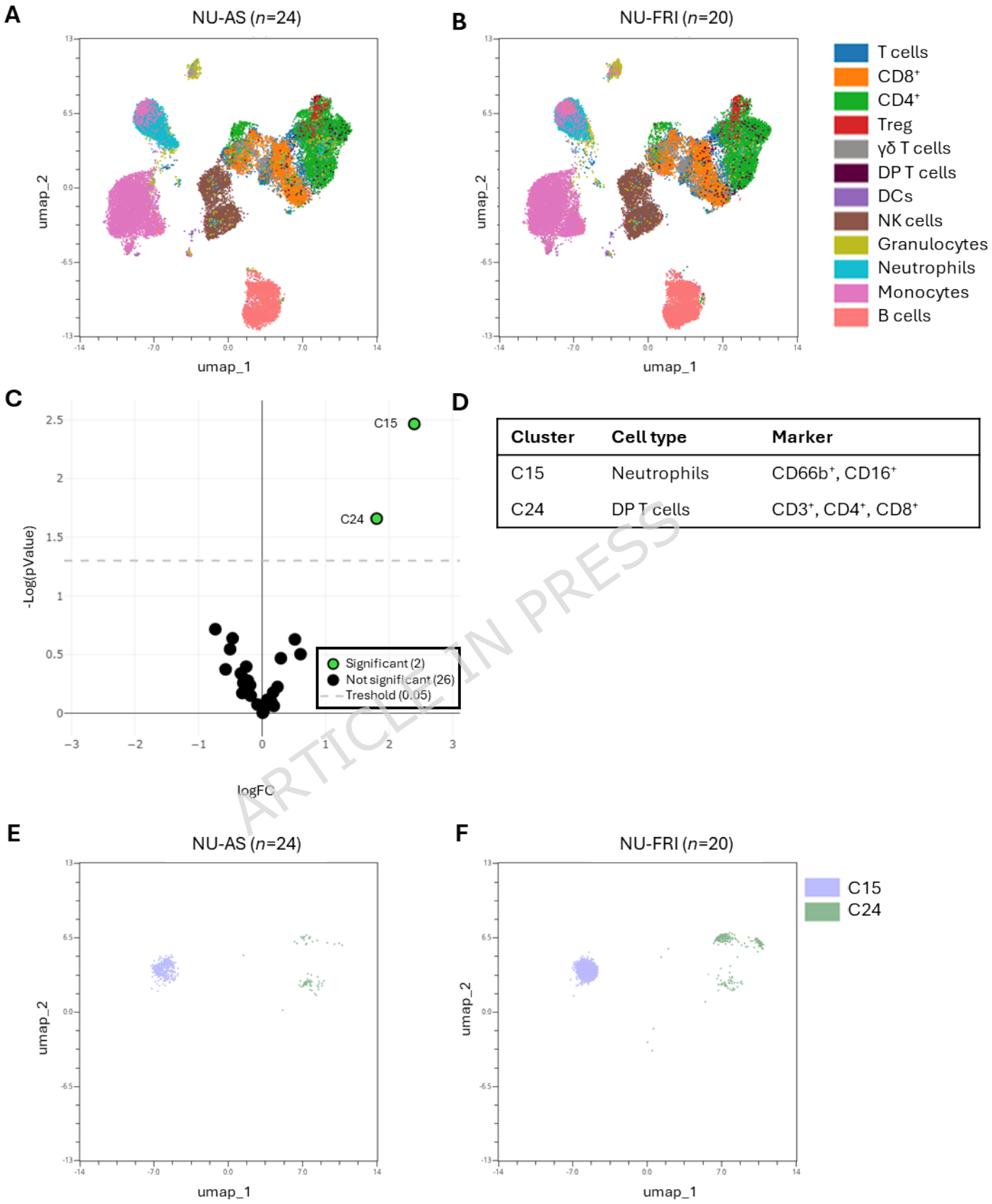

Cluster	Cell type	Marker
C15	Neutrophils	CD66b$^+$, CD16$^+$
C24	DP T cells	CD3$^+$, CD4$^+$, CD8$^+$

Figure 3: UMAP of PBMCs from NU-AS and NU-FRI patients. All cells from (A) NU-AS and (B) NU-FRI coloured by lineage. (C) Volcano plot comparing proportions of 28 metaclusters (MC) between

NU-AS and NU-FRI patients. The x-axis shows the difference in means of log2-transformed MC proportions; the y-axis shows the -log10-transformed Benjamini-Hochberg (BH)-adjusted p-value obtained using Welch's t-test. Green points above the horizontal line indicate significantly different clusters. (D) Significantly different clusters and with corresponding cell types and markers. UMAP representation of significantly different clusters in (E) NU-AS and (F) NU-FRI patients. Corresponding heatmaps are provided in Figure S1.

CD38$^+$ Tregs of NU-FRI are decreased in peripheral blood compared to NU-AS and H patients

T helper subsets were also analysed among H, NU-AS, and NU-FRI patients (Figure 4). Tregs (Figure 4A) and Th2 cells (Figure 4C) were increased in NU-AS compared to H (p=0.0163 and p=0.0421; respectively). Th1 cells were elevated in NU-FRI compared to H (p=0.0022; Figure 4B), and Th17 cells were increased in NU-AS compared to NU-FRI patients (p=0.0015; Figure 4D). Tfh cells were more abundant in H than NU-AS patients (p=0.0188; Figure 4E). CD38$^+$ CD4$^+$ T cells was significantly reduced in NU-AS compared to H patients (p=0.0010; Figure 4F), while CD38$^+$ Tregs were significantly lower in NU-FRI compared to both H and NU-

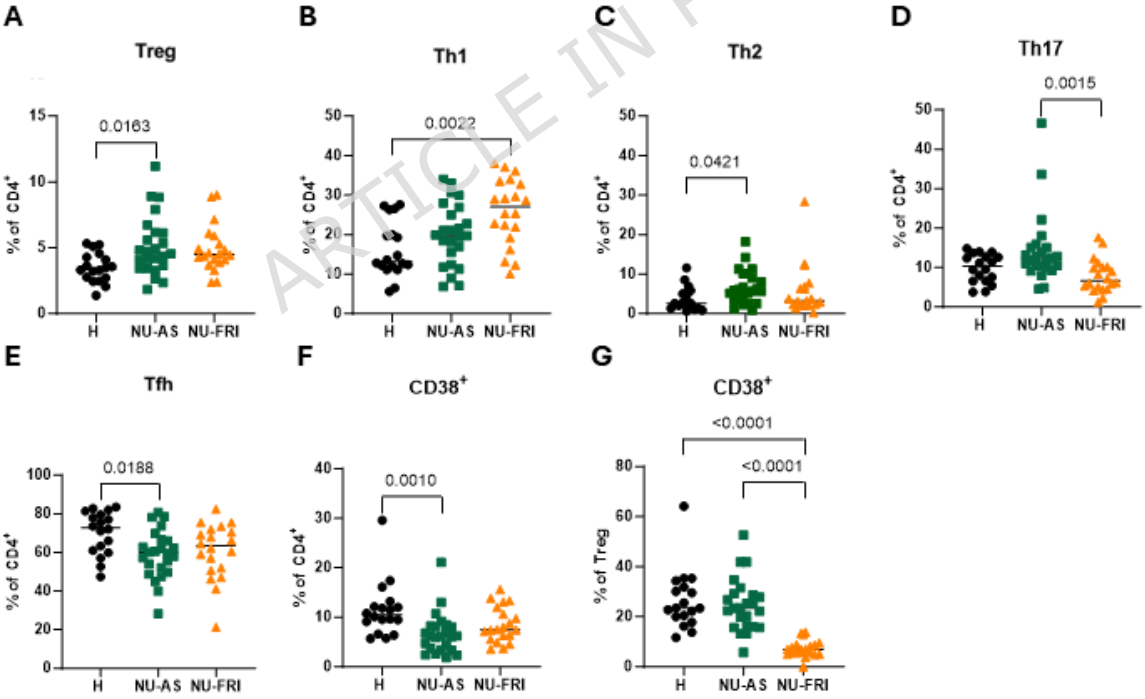

AS patients (p<0.0001 for both; Figure 4G).

Figure 4: **CD4$^+$ T helper subsets and CD38$^+$ cells in H, NU-AS, and NU-FRI patients.** (A) Tregs, (B) Th1 cells, (C) Th2 cells, (D) Th17 cells, and (E) Tfh cells, (F) CD38$^+$ CD4$^+$ T cells, and (G) CD38$^+$ Tregs in healed (H), NU-AS, and NU-FRI patients. Data shown are from individual patients (H: n=18; NU-AS: n=24; NU-FRI: n=20). Statistical analyses used one-way ANOVA or Kruskal-Wallis tests. Gating strategy: CD45$^+$CD66b$^-$, CD19$^-$CD20$^-$, CD3$^+$, CD4$^+$; Tregs: CCR4$^+$, CD45RA$^-$CD45RO$^+$,

CD127^{low}CD25^{high}; Th1: CD25^{-}, CXCR3^{+}CCR6^{-}; Th2: CD25^{-}, CXCR3^{-}CCR6^{-}; Th17: CD25^{-}, CXCR3^{-}CCR6^{+}; Tfh: CD25^{-}, CXCR3^{+}CCR6^{+}.

Monocytes in peripheral blood are elevated in NU-FRI compared to NU-AS and H patients

In addition to adaptive immune cells, our CyTOF panel enabled us to examine innate immune populations, given the observed differences between H and NU subgroups. Significant differences in monocyte abundance were also observed, with increased total monocytes levels in NU-FRI patients compared to H (p=0.0232) and NU-AS (p=0.0005) patients (Figure 5A). No significant differences were seen in classical (Figure 5B), non-classical (Figure 5C), or transitional monocyte subsets (Figure 5D).

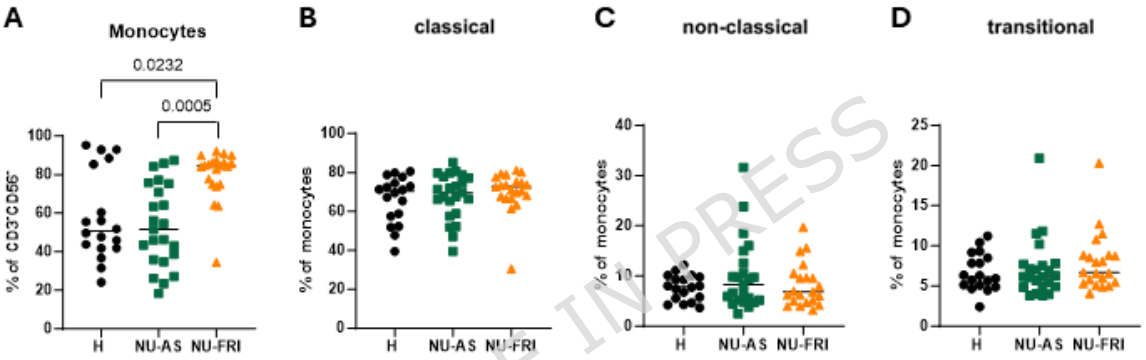

Figure 5: Monocytes and subsets in H, NU-AS, and NU-FRI patients. (A) Monocytes, (B) classical monocytes, (C) non-classical, and (D) transitional monocytes in healed (H), NU-AS, and NU-FRI patients. Data shown are from individual patients (H: n=18; NU-AS: n=24; NU-FRI: n=20). Statistical analyses used one-way ANOVA or Kruskal-Wallis tests. Gating strategy: Monocytes: CD45^{+}CD66b^{-}, CD19^{-}CD20^{-}, CD3^{-}CD56^{-}, CD14^{+}; classical: CD38^{+} CD14^{+}; non-classical: CD14^{low}, CD38^{-}; transitional: CD14^{+}, CD38^{low}.

Diagnostic potential of CD38^{+} Treg and monocyte counts

Given the distinct infection-induced changes in Tregs and Monocytes, we next assessed their potential as biomarkers of immune dysfunction. Receiver Operating Characteristic (ROC) analysis assessed the diagnostic potential of the counts of CD38^{+} Treg and monocyte fraction to distinguish NU-FRI from NU-AS (Figure 6A). The areas under the curve (AUC) were 0.965 for CD38^{+} Tregs and 0.808 for monocytes (Figure 6B). Combined analysis showed an AUC of 0.9965 and a high Youden index of 0.92 with a sensitivity of 100%, and a specificity of 91.7%.

A

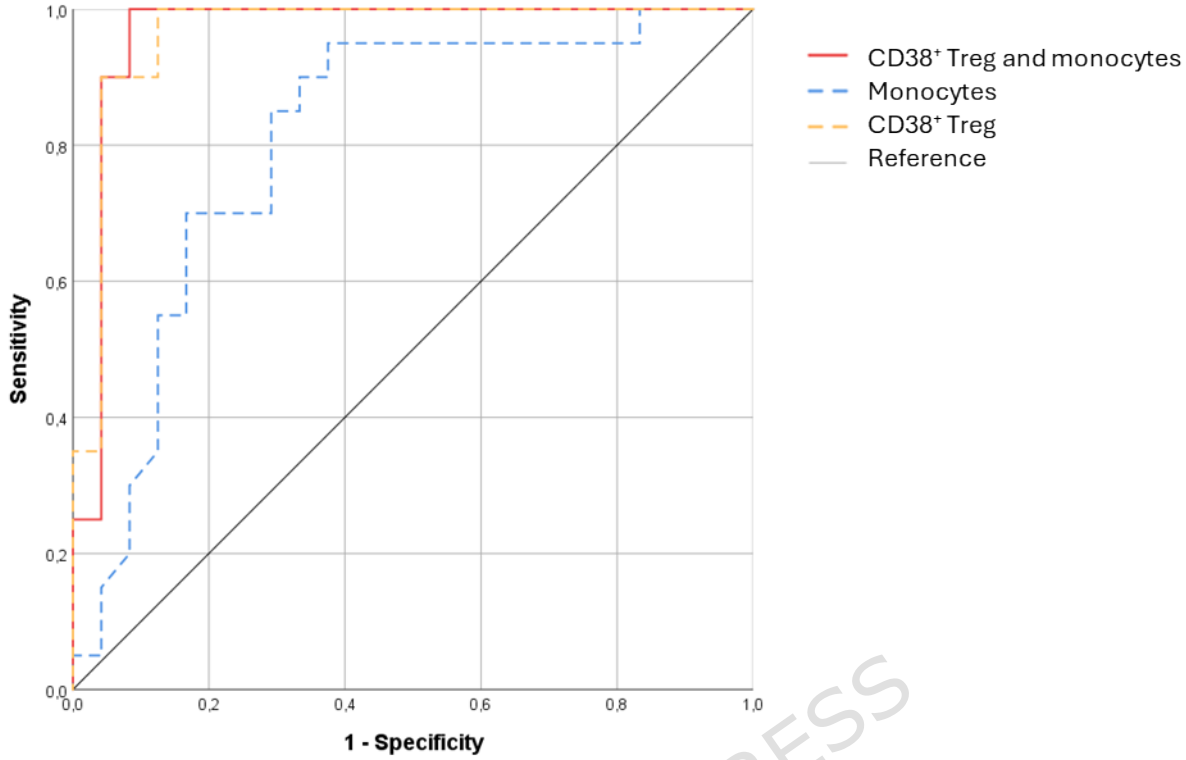

B

Biomarker	AUC (CI)	Youden Index	Cut-off	Sensitivity [%]	Specificity [%]
Monocytes	0.808 (0.675-0.942)	0.58	63.55 % of $CD3^{-}CD56^{-}$	95.0	62.5
$CD38^{+}$ Treg	0.965 (0.909-1.000)	0.88	14.70 % of Treg	100	87.5
$CD38^{+}$ Treg & monocytes	0.965 (0.903-1.000)	0.92	0.34	100	91.7

Figure 6: Receiver operating characteristic curve. (A) ROC curve for the discrimination of NU-AS and NU-FRI based on the number of monocytes and $CD38^{+}$ Treg cells, as well as their combination; (B) overview of the area under the ROC curve, the optimal cut-off at the maximum Youden index with the corresponding sensitivity and specificity for each biomarker.

Discussion

From a clinical perspective, managing fracture non-union (NU) is challenging due to its multifactorial nature and significantly different protocols dependent upon aetiology (infection or non-infectious reasons). Recent investigations have highlighted immune dysregulation as another potential factor. Impaired immune responses, possibly triggered or exacerbated by mechanical stress, may hinder bone regeneration and sustain chronic inflammation at fracture sites (8, 9, 34). Aside from providing insights into the biological and immunological processes underlying NU, there is also the potential for improved diagnostics by providing a more complete assessment of the systemic immune responses of patients with NU caused by infection or aseptic NU.

In this context, this is the first study to use samples from a large multicenter clinical study on NU to thoroughly investigate the underlying immune mechanisms associated with NU in humans. Initial comparisons comparing NU and H patients revealed substantial differences between these cohorts, with NU notably associated with increased Tregs. The elevated Treg levels in NU patients suggest an ongoing attempt to control inflammation and facilitate healing. In normal fracture healing, Tregs typically increase transiently, returning to baseline within one-month post-fracture (35). Previous studies have shown that patients with impaired mandibular fracture healing (as late as 6 months after surgery) exhibit a higher ratio of $CD8^+$ T effector to $CD4^+$ Treg ratio preoperatively, indicating an early immune dysregulation negatively impacting bone repair (26). Our cohort lacked preoperative samples after initial trauma for such comparison; however, at NU diagnosis, we did not observe this altered ratio (Figure S4K). In NU-FRI patients, persistent Treg activation may be driven by chronic antigen exposure, whereas in NU-AS patients it likely represents a response to sustained low-grade inflammation (21, 35, 36). It may be worth noting that, despite chronic antigenic exposure, exhaustion markers did not increase, indicating that immune suppression is more likely driven by Tregs than by T cell exhaustion. Since the prolonged elevation of Tregs was especially pronounced in NU-AS patients, this suggests that chronic infection was not the primary factor driving Treg expansion. The source of inflammation driving T reg persistence was not linked with diabetic or other known comorbidities but may at least in part be linked with mechanical instability. However, this cannot be reliably accounted for in the analysis of our outcomes but

may be more amenable to follow-up in a preclinical *in vivo* study where mechanics can be altered by implant fixation (8).

Crucially, we found fewer $CD38^+$ Tregs in NU patients compared to healed controls, which sub-group analysis revealed to be driven by the NU-FRI cohort. Typically, activated T cells upregulate CD38 expression during infection, which enhances proinflammatory cytokine production and promotes cell survival and maintains metabolism (27-29). Reduced CD38 expression in T cells in chronic inflammation is associated with impaired immune function and a diminished inflammatory response (27, 29). Our observation of more numerous reduced $CD38^+$ and, therefore, inactive Tregs in NU-FRI patients suggests impaired functionality or failure to resolve inflammation. However, it has been shown that that bone fracture leads to an increase in chemokines such as C-C motif chemokine ligand 22 (CCL22) at the fracture site (37, 38), which could orchestrate the selective recruitment and spatial reorganization of $CD38^+$ Tregs to the fracture zone, where they fine-tune inflammation and promote bone repair. This phenotype may hypothetically reflect excessive CCL22-driven recruitment to the fracture site, and this may likely indicate that local accumulation leads to a corresponding decrease in the periphery. This hypothesis may be addressed in future by investigations into CD38 marker expression in T cells at healing fracture sites.Another contrast to typical acute immune responses was the reduced Th17 cell levels in NU-FRI compared to NU-AS patients. Th17 cells typically defend against bacterial infections by promoting inflammation and coordinating broader immune responses (39, 40). Their reduction in NU-FRI might reflect again an increase at the site of infection or chronicity of infection. While Th17 cells drive pro-inflammatory responses, Tregs suppress them dependent on the cytokine environment. The relative balance between Tregs and Th17 cells is a critical determinant of the immune response. As Treg-associated cytokines (IL-10, TGF-β) inhibit IL-17, which is needed for Th17 differentiation (21, 41), reduced Th17 cell levels in NU-FRI compared to NU-AS patients could also be influenced by a higher number of (activated) Tregs. Measuring local tissue cytokine levels may aid in deciphering the precise local balance between Th17 and Tregs in non-union. The comparison between of NU-FRI to NU-AS patients showed a metaclusters of $CD4^+CD8^+$ T cells significantly elevated in NU-FRI compared to NU-AS. Double positive $CD4^+CD8^+$ T cells are often pro-inflammatory, show a T helper like phenotype, although they can also acquire cytotoxic functions. In chronic viral infections, rheumatoid arthritis, and graft-versus-host disease, these cells are

associated with increased pro-inflammatory responses and heightened tissue damage (42, 43). However, to date, the specific contribution of double-positive (DP) $CD4^+CD8^+$ T cells to bone infection and repair remains unexplored, as no studies have directly examined their functional role in fracture healing.

The prolonged elevation of Th1 cells observed in our NU cohort, especially in NU-FRI patients, indicates an ongoing inflammatory response driven by Th1-type immunity. Th1 cells are known to secrete proinflammatory cytokines which promotes cellular immune responses and contributes to tissue inflammation. However, during fracture healing, this prolonged Th1 dominance may contribute to a dysregulated immune environment that impairs tissue regeneration. By maintaining an inflammatory milieu, elevated Th1 activity may inhibit the resolution of inflammation and interfere with bone repair (44, 45). These findings support the notion that immune imbalance, rather than simple infection or mechanical factors alone, plays a pivotal role in the pathophysiology of non-union. A further finding from the sub-division of NU patients into FRI and NU-AS was a significant increase in monocytes in NU-FRI patients compared to NU-AS and H. Similar to Tregs, monocytes are key players in normal bone regeneration. Monocyte levels typically peak within the first few days following fracture and return to baseline within 2–4 weeks, depending on the progression and resolution of the remodelling phase (46-48). Persistently elevated monocyte levels, therefore, reflect abnormal inflammatory persistence. Our observation suggests chronic infection-driven inflammation in NU-FRI patients, potentially impeding the transition to bone formation. Thus, immune responses underlying NU differ substantially between NU-FRI (monocyte-driven) and NU-AS (Treg-mediated).

Clinically, distinguishing NU-FRI from NU-AS is essential, as their management significantly differs. NU-FRI management requires a staged surgical procedure, including surgical removal of the implant and eradication of the infection through resection and debridement combined with a systemic antibiotic therapy (1, 2). Only after the successful eradication of infection subsequent treatment of the non-union can be undertaken (49). NU-AS, on the other hand, is typically treated in a single-stage procedure using reamed intramedullary exchange nailing(50, 51). ROC curve analysis of $CD38^+$ Treg counts demonstrated strong potential for differentiating NU-FRI from NU-AS. High specificity and sensitivity, along with a high Youden index, suggest that $CD38^+$ Treg may be a potential biomarker for distinguishing infection-driven NU from aseptic cases. The discriminatory ability

was even higher when $CD38^+$ Treg counts were combined with monocyte counts. Currently, FRI diagnosis relies on both suggestive and confirmatory criteria, including preoperative parameters such as the patient's clinical presentation, serum inflammatory markers, and radiological imaging, as well as intraoperative microbiological and histopathological findings (52). However, a reliable preoperative diagnosis of FRI is not possible using these criteria and even the intraoperative diagnostics do not provide satisfactory sensitivity (53). Thus, immune profiling of monocytes and $CD38^+$ Tregs could significantly improve preoperative non-union diagnostics, enabling early targeted therapeutic interventions. Future, mechanistic studies would be of interest to determine of these cells suppress or activate inflammation, produce cytokines, or regulate repair. Functional assays would provide critical additional insights into T cell functionality, enabling additional understanding of the underlying biology as an adjunct the diagnostic potential. Interestingly, $CD38^+$ T cells are already used clinically as a biomarker in oncology, with their increased numbers being associated with disease progression in multiple myeloma patients (54), and similar testing facilities are presumably possible for routine diagnosis of NU-FRI. Overall, these results identify a promising preoperative biomarker for distinguishing infection-driven from aseptic NU, though validation in larger, independent cohorts is needed.

While our study provides a range of valuable insights into the immune landscape of NU patients that have not been previously described, several limitations should be acknowledged. The cohort size (62 patients) limits generalizability. Additionally, samples were collected at a single time point before surgical revision, and earlier or longitudinal sampling might offer greater insights. Given the logistical difficulties, acquiring larger cohorts or longitudinal samples remains challenging. It would also be advantageous to compare local immune profiles at the site of NU, which will likely contrast with the findings in the peripheral blood. PBMCs do offer a window into the involvement of immune cells in NU, however, local tissue samples would also be desirable. Of course, matched bone samples from healthy healed patients may not be easy to acquire, leading to lack of important control tissues in such circumstances. As open fractures are a recognized risk factor for the development of FRI (55), it is not surprising that this association is also observed in FRI occurring in late-stage non-union. Consequently, our study showed also that the healed patient group displayed a significant lower percentage of open fractures and a lower percentage of plate fixations. However, because of the small

sample size, a subgroup analysis based on implant used or bone affected was not possible. Furthermore, our study primarily focused on immune phenotyping rather than functional assays such as cytokine production or proliferation tests, which might provide further mechanistic insights We also observed discrepancies between UMAP, and statistical analysis may mask differences within specific cell clusters, such as γδ T cell cluster, due to aggregating multiple distinct subsets.

Conclusions

Despite limitations, this study significantly advances understanding of immune mechanisms underlying fracture NU and identified potentially clinically relevant diagnostic biomarkers. This represents the first application of high-dimensional mass cytometry (CyTOF) to NU patients, enabling comprehensive immune profiling, far surpassing conventional flow cytometry approaches in depth and detail. Future research should explore mechanistic roles of Th1, Th2, and Treg cells in fracture healing and NU, along mechanisms sustaining monocyte elevation and CD38 expression over time in NU-FRI.

NU patients exhibit distinct T helper subsets compared to healed patients. While differentiating FRI from aseptic NU clinically remains challenging due to subtle clinical signs, immune characterization provides new insights into the nuanced immune landscape of NU fractures. Importantly, our study identified distinct immune biomarkers with clinical potential to differentiate NU-FRI from NU-AS, potentially aiding future diagnostics and patient management.

Methods

Patient cohort

This prospective multicenter clinical study characterised immune cell phenotypes in the peripheral blood from patients with aseptic non-union (NU-AS) and fracture-related infected non-union (NU-FRI), comparing them to patients with complication-free fracture healing outcomes (H). More than one hundred patients were enrolled at eight level-I trauma centers in Germany between January 2019 and April 2022 (56). After matching for gender and age between the groups, 62 patients from whom at least 5×10^6 PBMCs could be isolated from preoperative peripheral blood samples were included in this analysis (Figure 7). The study was approved by the Ethics Committee of the Institutional and National Medical Board (Bavarian State Chamber of Physicians, ID 2016-16041, initial vote) and registered in the German Clinical Trails Register and WHO International Clinical Trial Registry Platform (DRKS00014657, https://trialsearch.who.int/Trial2.aspx?TrialID=DRKS00014657, first date of registration 26/04/2018). Each of the 8 study centers obtained local ethical approval (secondary votes: BG Klinikum Duisburg: Ethik-Kommission der Ärztekammer Nordrhein (approval number: 2018285), BG Unfallklinik Frankfurt am Main: Ethik-Kommission bei der Landesärztekammer Hessen (approval number: MC 112/2018), BG Unfallklinik Ludwigshafen: Ethik-Kommission der Landesärztekammer Rheinland-Pfalz (approval number: 2018-13316-Klinische Forschung), BG Klinik Tübingen: Ethik-Kommission an der Medizinischen Fakultät der Eberhard-Karls-Universität und am Universitätsklinikum Tübingen (approval number: 722/2016BO2), BG Klinikum Bergmannstrost Halle: Ethikkommission der Ärztekammer Sachsen-Anhalt (approval number: 33/18) and BG Klinikum Hamburg Ethik-Kommission der Ärztekammer Hamburg (approval number: MC-184/18), BG Klinikum Unfallkrankenhaus Berlin did not require a secondary vote from its local ethics committee, the initial vote of Ethik-Kommission der

Bayerischen Landesärztekammer (approval number: 16041) was sufficient) and

A

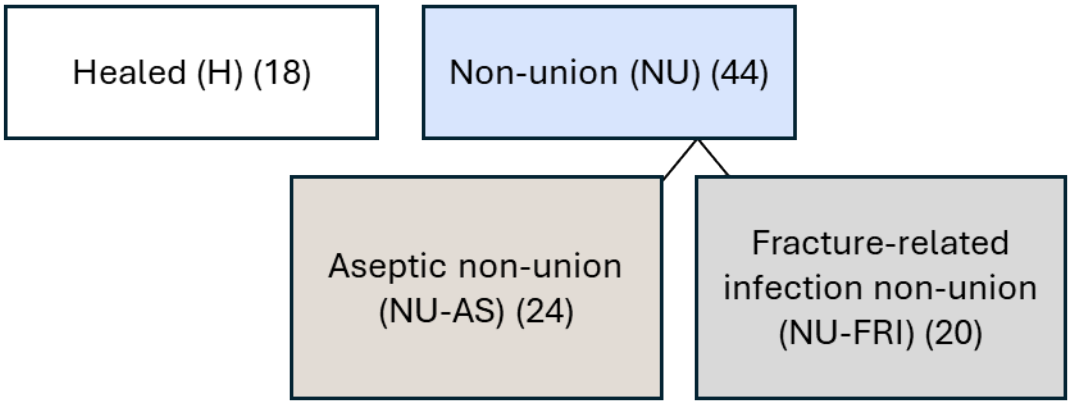

B

Group (number of patients)	H (18)	NU (44)	NU-AS (24)	NU-FRI (20)
% female	27.7%	29.5%	37.5%	25%
Age	41.2±16.2	50.4±17.2	53.6±17.1	46.6±16
BMI	22.9±2.2	28.1±5.7	27.8±5.9	28.3±5.4
Diabetes patients	0%	18%	12.5%	25%
Smoker	22%	9%	12.5%	5%
Polytrauma (no/ yes)	94.4%/ 5.6%	81.8%/ 18.2%	83.3%/ 16.7%	80%/ 20%
Fracture (open/ closed)	16.6%/ 83.4%	52.2%/ 47.8%	17.2%/ 82.2%	50%/ 50%
Bone (Tibia/ Femur)	77.8%/ 22.2%	61.4%/ 38.4%	50%/ 50%	75%/ 25%
Treatment procedure (Plate/ Intramedullary nail)	5.6%/ 94.4%	38.4%/ 61.4%	33.3%/ 66.6%	45%/ 55%
Time between fracture stabilization and non-union revision (days)	-	454.7 (94-1334)	412.5 (162-1254)	505.5 (94-1334)

all patients provided written informed consent before inclusion.

Figure 7: Group assignment, and clinical data. (A NU patients sub-divided into NU-AS and NU-FRI.(B) Summary of clinical data of included patients.

Peripheral heparinized blood (Plus Blood Collection Tubes, BD Vacutainer, Plymouth, UK) was collected preoperatively from patients with femoral or tibial shaft non-union requiring revision surgery (index surgery), as well as from patients

with healed femoral or tibial fractures undergoing implant removal, who served as controls. Non-union was diagnosed based on clinical symptoms, clinical evaluation, and radiographic assessment. Radiographic criteria for non-union included the absence of a bony bridge in at least three out of four cortices on anteroposterior and lateral views of conventional radiographs (57). Consequently, non-union was defined as a fracture failing to heal without additional surgical intervention (5). In the healed group, implants were removed after complication-free fracture consolidation, without clinical or laboratory signs of infection or delayed healing. Exclusion criteria, previously described by Trenkwalder *et al.*, 2025 (56), included long-term antibiotic use before surgery, ongoing antimicrobial treatment, pregnancy, acute infection of other origins, simultaneous non-union at different sites, immunosuppression, autoimmune disease, or malignancy.

NU-FRI was diagnosed according to the diagnostic criteria for FRI (1, 58), including the presence of a fistula, identification of the same pathogen in two separate tissue cultures, detection of the same pathogen in both tissue culture and sonication fluid, or identification of microorganisms in a single tissue culture confirmed by histopathology. Cases with only one positive tissue or sonication culture were classified as NU-AS (56). Histopathological evidence alone (Histopathological Osteomyelitis Evaluation Score; HOES) was insufficient to confirm infection, as previously described (59). NU diagnosis (AS or FRI) was based on microbiological and histopathological findings from the index surgery and any subsequent surgeries within 12 months of inclusion. On average, 4.5 (IQR 3–6) samples for microbiological analysis (including tissue cultures and sonication, if available) and 1 (IQR 1–2) sample for histopathology were collected during revision surgery for infection diagnostics.

In total, 18 healed (H) patients and 44 NU patients were included (Figure 7A). NU patients were divided into NU-AS (n=24) and NU-FRI (n=20). Clinical data including sex, age, body mass index (BMI), diabetes, and smoking status as well as injury and fixation details (polytrauma, affected bone, implant used and injury type) are summarized in Figure 7B. NU patients had more open fractures (52%) compared the healed patients (16.6%), however, this was due to the high rate of open fractures in FRI patients (50%), while AS patients had an open fracture rate (17.2%) similar to the healed patients. Plating fixation was lowest in the healed cohort (5.6%), while it was elevated in both the NU-AS (33.3%) and NU-FRI (45%) cohort.

A chi-square test showed that the healed patient group displayed a significant lower percentage of open fractures and a lower percentage of plate fixations (p=0.375, p=0.0331, respectively). It is recognised that open fractures are a risk factor for developing FRI (55). and this is also observed in the FRI associated with later stage non-union. To add is that non-union is diagnosed after 6 to 9 months and the revision is considered on a case-by-case basis as needed. Not all patients are in the early post-fracture phase, as all were diagnosed at least 94 days after fracture stabilization. NU patients ranged from 94 days to 1334 days, NU-AS from 162 days to 1254 days and NU-FRI from 94 days to 1334 days. The non-union revision was, on average, 93 days earlier in NU-AS patients than in NU-FRI patients, but the difference was not significant.

Isolation of PBMCs

PBMCs were isolated from peripheral blood by density gradient centrifugation. Heparinized blood was diluted with Dulbecco's phosphate-buffered saline (DPBS; Bio&SELL GmbH, Germany). The blood-DPBS mixture was layered over BioColl separation medium (Bio&SELL GmbH, Germany) in separation tubes (Kisker Biotech GmbH & Co. KG., Germany). After centrifugation (800 × *g*, 20 min, room temperature (RT)), the PBMC layer was washed first with DPBS (500 × *g*, 10 min, RT), then with complete Roswell Park Memorial Institute Medium (cRPMI: RPMI supplemented with 10 % fetal calf serum (FCS); 300 × *g*, 10 min, RT). PMBC pellets were resuspended in cRPMI, and viable cell counts were determined using trypan blue (0.4%, Sigma-Aldrich, USA) and a Neubauer improved counting chamber (Karl Hecht GmbH & Co KG, Germany).

Cells were cryopreserved in cold freezing medium (20% DMSO/FCS) at 5-35 × 10^6 cells/mL, frozen overnight at -80 °C in Mr. Frosty freezing containers (Thermo Fisher Scientific, USA) containing 2-propanol (AppliChem GmbH, Germany), and stored in liquid nitrogen until use.

Antibody labelling and titration

Antibodies were conjugated with lanthanide and cadmium metals using Maxpar Antibody Labeling Kits (Fluidigm, USA) according to the manufacturer's instructions. Cadmium-labelled antibodies were eluted in W-buffer (Fluidigm) and HRP-Protector peroxidase stabilizer; lanthanide-labelled antibodies were eluted in W-buffer (Fluidigm) and antibody stabilizer buffer (Candor Bioscience, Germany) supplemented with 0.05% sodium azide. The final antibody volume was adjusted by adding an equal volume of antibody stabilizer buffer (Fluidigm; supplemented with 0.05% sodium azide or HRP-Protector). Antibodies were stored at 4 °C. All antibodies were titrated on healthy donor PBMCs to determine optimal staining concentrations (Table S1).

Antibody staining

Cryopreserved PBMCs were thawed and stained in batches using an immune profiling kit (Standard BioTools, USA) supplemented with additional conjugated antibodies (Table S1). PBMCs were incubated with Human TruStain FcX (BioLegend, USA) for 10 min at RT to block Fc receptors (FcR). After centrifugation (300 × *g*, 5 min), cells were stained with metal-conjugated antibodies for 30 min at RT. After staining, cells were washed twice with Maxpar® Cell Staining Buffer (CSB; Fluidigm; 300 × *g*, 5 min), fixed with 1.6% formaldehyde solution (Thermo Fisher Scientific) for 10 min at RT, and centrifuged (800 × *g*, 5 min). Cells were then incubated in 250 µM Cell-ID™ Intercalator-Ir (Fluidigm) in Maxpar Fix and Perm Buffer (Fluidigm) overnight at 4 °C. The next day, cells were centrifuged (800 × *g*, 5 min), resuspended in 100 µL residual volume, and frozen at -80 °C until acquisition.

Data acquisition

Cells were washed twice with CSB and cell acquisition solution (CAS; Fluidigm), filtered through a 35 µm cell strainer, and mixed with EQ Four Element Calibration Beads (Fluidigm). Acquisition was performed on a Helios™ mass cytometer (Fluidigm) at 250–300 events/second. Data normalization was done using EQ beads. Samples were acquired across eight days, mixing patient groups to minimize batch effects.

Data processing and analysis

Data were analysed using FlowJo V10 (Treestar, USA) and GraphPad Prism 10 (GraphPad Software Inc., USA). Gating strategy can be found in the supplements (Figure S9-S13). Statistical analyses included Mann-Whitney U test or Welch's tests (H *vs* NU), and one-way ANOVA with Tukey's multiple comparisons or Kruskal-Wallis tests (H *vs* NU-AS *vs* NU-FRI), depending on normality distribution testing. Significance was set at $p<0.05$.

Normalized data was uploaded to OMIQ (OMIQ, USA) and an arcsinh transformation with a coefficient of 5 was applied. A standardized cleanup strategy, as described by Bagwell *et al.*, 2020 (60), was applied. Further analysis was performed on the transformed data. Data consistency was evaluated over time; non-conforming sections were gated out using flowCut. Viable $CD45^+$ single cells were selected by manual gating. For lineage population analysis, total live $CD45^+$ single cells were down-sampled to 2,000 events per subject. Unsupervised analysis employed uniform manifold approximation and projection (UMAP; neighbours=15, minimum

distance=0.4, components=2; metric=Euclidean, embedding initialization=spectral), followed by PhenoGraph clustering (k=100). Significant cluster differences were identified using EdgeR (OMIQ) or visualized as heatmaps with Euclidean clustering. Metacluster proportions were analysed by Welch's t-test with Benjamini-Hochberg (BH)-adjusted p-values.

Immunological parameters distinguishing NU-FRI from NU-AS were evaluated using receiver operating characteristic (ROC) curve analysis in SPSS (ver. 26; IBM, USA). Optimal cut-off values, sensitivity, and specificity were determined using the maximum Youden index. A ROC curve combining two predictors was generated based on binary logistic regression predictive probabilities.

Availability of data and materials

The datasets used and/or analysed during the current study are available from the corresponding author on reasonable request.

Ethics approval and consent to participate

This study was conducted in accordance with the Declaration of Helsinki. The study was approved by the Ethics Committee of the Institutional and National Medical Board (Bavarian State Chamber of Physicians, ID 2016-16041). Each study center received an ethics vote from its local responsible ethics committee. All patients provided their written consent before study inclusion.

Competing interests

The authors declare that they have no known competing financial interests or personal relationships that could have appeared to influence the work reported in this paper.

Funding

The study was supported by the German Social Accident Insurance, DGUV grant number FF-FR 0276 and AO Trauma grant number AR_2021_08.

Authors contributions

P.F.: Data collection, data curation, data visualization, manuscript writing, manuscript revision; **C.S., TF.M:** supervision; **K.T. and S.E.:** PBMC isolation; **P.F., C.S., K.T., S.E., S.H., F.W., G.M., CA.A., M.R., JJ.GV., G.M.**, **SAJ.Z., TF.M., EC.dJ:** manuscript revision; **K.T. and S.E; S.H.:** Conceptualization and implementation of the multicenter study**; F.W.**: Recruitment of patients, patient survey collection, **G.M.**, **SA.JZ., EC.dJ:** Data interpretation, **CA.A., M.R.:** Input on data Interpretation, **J.J.GV.:** Supervision for data analysis and data visualization; **S.H., SAJ.Z., EC.dJ., TF.M.:** funding

Acknowledgement

We would like to thank Beate Rückert and Laura Bürgi (Swiss Institute of Allergy and Asthma Research Davos (SIAF)) for technical support with the CyTOF Helios. We also thank the Septic Aseptic Nonunion Differentiation (SAND) Research Group for patient recruitment and samples collection: *Berufsgenossenschaftliche Unfallklinik Murnau:* Matthias Militz, Simon Hackl, Ferdinand Weisemann,

Katharina Trenkwalder, Sandra Erichsen, Tobias Hentschel, Peter Augat; *Berufsgenossenschaftliche Klinik Tübingen:* Heiko Baumgartner, Marie Reumann; *Berufsgenossenschaftliche Klinik Ludwigshafen:* Georg Reiter, Holger Freischmidt; *Berufsgenossenschaftliche Unfallklinik Frankfurt:* Matthias Kemmerer; *Berufsgenossenschaftliches Klinikum Bergmannstrost Halle:* Steffen Langwald, John Hanke; *Berufsgenossenschaftliches Klinikum Duisburg:* Martin Glombitza, Eva Steinhausen; *Berufsgenossenschaftliches Klinikum Hamburg:* Ulf-Joachim Gerlach; *Berufsgenossenschaftliches Klinikum Unfallkrankenhaus Berlin:* Nikolai Spranger; *Berufsgenossenschaftliche Kliniken – Klinikverbund:* Dirk Stengel.

References

1. Moriarty TF, Metsemakers W-J, Morgenstern M, Hofstee MI, Vallejo Diaz A, Cassat JE, et al. Fracture-related infection. Nature Reviews Disease Primers. 2022;8(1):67.
2. Metsemakers WJ, Moriarty TF, Morgenstern M, Marais L, Onsea J, O'Toole RV, et al. The global burden of fracture-related infection: can we do better? Lancet Infect Dis. 2024;24(6):e386-e93.
3. Meinberg EG, Clark D, Miclau KR, Marcucio R, Miclau T. Fracture repair in the elderly: Clinical and experimental considerations. Injury. 2019;50 Suppl 1(Suppl 1):S62-s5.
4. Stewart SK. Fracture Non-Union: A Review of Clinical Challenges and Future Research Needs. Malays Orthop J. 2019;13(2):1-10.
5. Schmidmaier G, Moghaddam A. [Long Bone Nonunion]. Z Orthop Unfall. 2015;153(6):659-74; quiz 75-6.
6. Hak DJ, Fitzpatrick D, Bishop JA, Marsh JL, Tilp S, Schnettler R, et al. Delayed union and nonunions: epidemiology, clinical issues, and financial aspects. Injury. 2014;45 Suppl 2:S3-7.
7. Siverino C, Metsemakers WJ, Sutter R, Della Bella E, Morgenstern M, Barcik J, et al. Clinical management and innovation in fracture non-union. Expert Opin Biol Ther. 2024;24(9):973-91.
8. Sabaté-Brescó M, Berset CM, Zeiter S, Stanic B, Thompson K, Ziegler M, et al. Fracture biomechanics influence local and systemic immune responses in a murine fracture-related infection model. Biol Open. 2021;10(9).
9. Zhang E, Miramini S, Patel M, Richardson M, Ebeling P, Zhang L. The effects of mechanical instability on PDGF mediated inflammatory response at early stage of fracture healing under diabetic condition. Comput Methods Programs Biomed. 2023;229:107319.
10. Impieri L, Pezzi A, Hadad H, Peretti GM, Mangiavini L, Rossi N. Orthobiologics in delayed union and non-union of adult long bones fractures: A systematic review. Bone Reports. 2024;21:101760.
11. Lv S, Wang G, Dai L, Wang T, Wang F. Cellular and Molecular Connections Between Bone Fracture Healing and Exosomes. Physiol Res. 2023;72(5):565-74.
12. Maruyama M, Rhee C, Utsunomiya T, Zhang N, Ueno M, Yao Z, et al. Modulation of the Inflammatory Response and Bone Healing. Front Endocrinol (Lausanne). 2020;11:386.
13. Baht GS, Vi L, Alman BA. The Role of the Immune Cells in Fracture Healing. Current Osteoporosis Reports. 2018;16(2):138-45.
14. Burgan J, Rahmati M, Lee M, Saiz AM. Innate immune response to bone fracture healing. Bone. 2025;190:117327.
15. Chow SK, Wong CH, Cui C, Li MM, Wong RMY, Cheung WH. Modulating macrophage polarization for the enhancement of fracture healing, a systematic review. J Orthop Translat. 2022;36:83-90.
16. Koh TJ, DiPietro LA. Inflammation and wound healing: the role of the macrophage. Expert Rev Mol Med. 2011;13:e23.
17. Sato K, Suematsu A, Okamoto K, Yamaguchi A, Morishita Y, Kadono Y, et al. Th17 functions as an osteoclastogenic helper T cell subset that links T cell activation and bone destruction. J Exp Med. 2006;203(12):2673-82.
18. Yang N, Liu Y. The Role of the Immune Microenvironment in Bone Regeneration. Int J Med Sci. 2021;18(16):3697-707.
19. Liu Y, Wang L, Liu S, Liu D, Chen C, Xu X, et al. Transplantation of SHED prevents bone loss in the early phase of ovariectomy-induced osteoporosis. J Dent Res. 2014;93(11):1124-32.

20. Wang H, Li Y, Li H, Yan X, Jiang Z, Feng L, et al. T cell related osteoimmunology in fracture healing: Potential targets for augmenting bone regeneration. Journal of Orthopaedic Translation. 2025;51:82-93.
21. Wu T, Wang L, Jian C, Zhang Z, Zeng R, Mi B, et al. A distinct “repair” role of regulatory T cells in fracture healing. Frontiers of Medicine. 2024;18(3):516-37.
22. Xu F, Guanghao C, Liang Y, Jun W, Wei W, Baorong H. Treg-promoted New Bone Formation Through Suppressing TH17 by Secreting Interleukin-10 in Ankylosing Spondylitis. Spine (Phila Pa 1976). 2019;44(23):E1349-e55.
23. Zhang W, Dang K, Huai Y, Qian A. Osteoimmunology: The Regulatory Roles of T Lymphocytes in Osteoporosis. Front Endocrinol (Lausanne). 2020;11:465.
24. Wang D, Taylor GM, Gilbert JR, Losee JE, Sodhi CP, Hackam DJ, et al. Enhanced Calvarial Bone Healing in CD11c-TLR4-/- and MyD88-/- Mice. Plast Reconstr Surg. 2017;139(4):933e-40e.
25. Georgiev P, Benamar M, Han S, Haigis MC, Sharpe AH, Chatila TA. Regulatory T cells in dominant immunologic tolerance. J Allergy Clin Immunol. 2024;153(1):28-41.
26. Voss JO, Pivetta F, Elkilany A, Schmidt-Bleek K, Duda GN, Odaka K, et al. Prognostic implications of a CD8+ TEMRA to CD4+Treg imbalance in mandibular fracture healing: a prospective analysis of immune profiles. Frontiers in Immunology. 2024;15.
27. Ghosh A, Khanam A, Ray K, Mathur P, Subramanian A, Poonia B, et al. CD38: an ecto-enzyme with functional diversity in T cells. Frontiers in Immunology. 2023;Volume 14 - 2023.
28. Glaría E, Valledor AF. Roles of CD38 in the Immune Response to Infection. Cells. 2020;9(1):228.
29. Kar A, Mehrotra S, Chatterjee S. CD38: T Cell Immuno-Metabolic Modulator. Cells. 2020;9(7).
30. DeRogatis JM, Neubert EN, Viramontes KM, Henriquez ML, Nicholas DA, Tinoco R. Cell-Intrinsic CD38 Expression Sustains Exhausted CD8(+) T Cells by Regulating Their Survival and Metabolism during Chronic Viral Infection. J Virol. 2023;97(4):e0022523.
31. Yang S, Ding W, Feng D, Gong H, Zhu D, Chen B, et al. Loss of B cell regulatory function is associated with delayed healing in patients with tibia fracture. Apmis. 2015;123(11):975-85.
32. Molitoris KH, Huang M, Baht GS. Osteoimmunology of Fracture Healing. Current Osteoporosis Reports. 2024;22(3):330-9.
33. Sun G, Wang Y, Ti Y, Wang J, Zhao J, Qian H. Regulatory B cell is critical in bone union process through suppressing proinflammatory cytokines and stimulating Foxp3 in Treg cells. Clin Exp Pharmacol Physiol. 2017;44(4):455-62.
34. Duda GN, Geissler S, Checa S, Tsitsilonis S, Petersen A, Schmidt-Bleek K. The decisive early phase of bone regeneration. Nature Reviews Rheumatology. 2023;19(2):78-95.
35. Griffith JW, Luster AD. No bones about it: regulatory T cells promote fracture healing. J Clin Invest. 2025;135(2).
36. Taams LS, Palmer DB, Akbar AN, Robinson DS, Brown Z, Hawrylowicz CM. Regulatory T cells in human disease and their potential for therapeutic manipulation. Immunology. 2006;118(1):1-9.
37. Glowacki AJ, Yoshizawa S, Jhunjhunwala S, Vieira AE, Garlet GP, Sfeir C, et al. Prevention of inflammation-mediated bone loss in murine and canine periodontal disease via recruitment of regulatory lymphocytes. Proceedings of the National Academy of Sciences. 2013;110(46):18525-30.
38. Borrelli MA, Warunek JJ, Little SR, Turnquist HR. Regulatory T Cell Attracting Therapy Accelerates Skeletal Muscle Functional Recovery Following Injury. Res Sq. 2025.

39. Paroli M, Caccavale R, Fiorillo MT, Spadea L, Gumina S, Candela V, et al. The Double Game Played by Th17 Cells in Infection: Host Defense and Immunopathology. Pathogens. 2022;11(12):1547.
40. Li Y, Wei C, Xu H, Jia J, Wei Z, Guo R, et al. The Immunoregulation of Th17 in Host against Intracellular Bacterial Infection. Mediators Inflamm. 2018;2018:6587296.
41. Leung S, Liu X, Fang L, Chen X, Guo T, Zhang J. The cytokine milieu in the interplay of pathogenic Th1/Th17 cells and regulatory T cells in autoimmune disease. Cell Mol Immunol. 2010;7(3):182-9.
42. Hess NJ, Turicek DP, Riendeau J, McIlwain SJ, Contreras Guzman E, Nadiminti K, et al. Inflammatory CD4/CD8 double-positive human T cells arise from reactive CD8 T cells and are sufficient to mediate GVHD pathology. Sci Adv. 2023;9(12):eadf0567.
43. Quandt D, Rothe K, Scholz R, Baerwald CW, Wagner U. Peripheral CD4CD8 Double Positive T Cells with a Distinct Helper Cytokine Profile Are Increased in Rheumatoid Arthritis. PLOS ONE. 2014;9(3):e93293.
44. Dardalhon V, Korn T, Kuchroo VK, Anderson AC. Role of Th1 and Th17 cells in organ-specific autoimmunity. J Autoimmun. 2008;31(3):252-6.
45. Chen J, Xiang X, Nie L, Guo X, Zhang F, Wen C, et al. The emerging role of Th1 cells in atherosclerosis and its implications for therapy. Frontiers in Immunology. 2023;Volume 13 - 2022.
46. Landén NX, Li D, Ståhle M. Transition from inflammation to proliferation: a critical step during wound healing. Cell Mol Life Sci. 2016;73(20):3861-85.
47. Ogle ME, Segar CE, Sridhar S, Botchwey EA. Monocytes and macrophages in tissue repair: Implications for immunoregenerative biomaterial design. Exp Biol Med (Maywood). 2016;241(10):1084-97.
48. Muire PJ, Mangum LH, Wenke JC. Time Course of Immune Response and Immunomodulation During Normal and Delayed Healing of Musculoskeletal Wounds. Frontiers in Immunology. 2020;Volume 11 - 2020.
49. Simpson AH, Tsang JST. Current treatment of infected non-union after intramedullary nailing. Injury. 2017;48:S82-S90.
50. Hierholzer C, Friederichs J, Glowalla C, Woltmann A, Bühren V, von Rüden C. Reamed intramedullary exchange nailing in the operative treatment of aseptic tibial shaft nonunion. Int Orthop. 2017;41(8):1647-53.
51. Hierholzer C, Glowalla C, Herrler M, von Rüden C, Hungerer S, Bühren V, et al. Reamed intramedullary exchange nailing: treatment of choice of aseptic femoral shaft nonunion. J Orthop Surg Res. 2014;9:88.
52. Govaert GAM, Kuehl R, Atkins BL, Trampuz A, Morgenstern M, Obremskey WT, et al. Diagnosing Fracture-Related Infection: Current Concepts and Recommendations. J Orthop Trauma. 2020;34(1):8-17.
53. Trenkwalder K, Hackl S, Weisemann F, Augat P. The value of current diagnostic techniques in the diagnosis of fracture-related infections: Serum markers, histology, and cultures. Injury. 2024;55 Suppl 6:111862.
54. Chen H, Wang X, Wang Y, Chang X. What happens to regulatory T cells in multiple myeloma. Cell Death Discovery. 2023;9(1):468.
55. Coombs J, Billow D, Cereijo C, Patterson B, Pinney S. Current Concept Review: Risk Factors for Infection Following Open Fractures. Orthop Res Rev. 2022;14:383-91.
56. Trenkwalder K, Erichsen S, Weisemann F, von Rüden C, Augat P, Sand Research G, et al. Low-grade infections in nonunion of the femur and tibia without clinical suspicion of infection - Incidence, microbiology, treatment, and outcome. Injury. 2025;56(2):112137.
57. Fisher JS, Kazam JJ, Fufa D, Bartolotta RJ. Radiologic evaluation of fracture healing. Skeletal Radiol. 2019;48(3):349-61.

58. Metsemakers WJ, Morgenstern M, McNally MA, Moriarty TF, McFadyen I, Scarborough M, et al. Fracture-related infection: A consensus on definition from an international expert group. Injury. 2018;49(3):505-10.
59. Trenkwalder K, Erichsen S, Weisemann F, Augat P, Militz M, von Rüden C, et al. The value of sonication in the differential diagnosis of septic and aseptic femoral and tibial shaft nonunion in comparison to conventional tissue culture and histopathology: a prospective multicenter clinical study. J Orthop Traumatol. 2023;24(1):25.
60. Bagwell CB, Inokuma M, Hunsberger B, Herbert D, Bray C, Hill B, et al. Automated Data Cleanup for Mass Cytometry. Cytometry A. 2020;97(2):184-98.

Figure legends

Figure 1: Uniform manifold approximation and projection (UMAP) of PBMCs from all Healed and Non-union patients. UMAP representation of all cells from (A) H and (B) NU patients coloured by lineage. (C) Volcano plot comparing proportions of 28 metaclusters (MC) between H and NU patients. The x-axis shows the difference in means of log2-transformed MC proportions; the y-axis shows the -log10-transformed Benjamini-Hochberg (BH)-adjusted p-value obtained using Welch's t-test. Green points above the horizontal line indicate significantly different clusters. Downregulated clusters are marked in grey. (D) Significantly different clusters with corresponding cell types and markers. UMAP representation of significantly different clusters in (E) H and (F) NU patients. Corresponding heatmaps are provided in Figure S1.

Figure 2: $CD4^+$ T helper subsets and $CD38^+$ cells in Healed versus Non-union patients. (A) Tregs, (B) Th1 cells, (C) Th2 cells, (D) Tfh cells, (E) $CD38^+$ $CD4^+$ T cells, and (F) $CD38^+$ Tregs. Data shown are from individual patients (H: n=18; NU: n=44). Statistical analyses performed used Mann-Whitney or Welch's tests. Gating strategy: $CD45^+CD66b^-$, $CD19^-CD20^-$, $CD3^+$, $CD4^+$; Tregs: $CCR4^+$, $CD45RA^-CD45RO^+$, $CD127^{low}CD25^{high}$; Th1 cells: $CD25^-$, $CXCR3^+CCR6^-$; Th2 cells: $CD25^-$, $CXCR3^-CCR6^-$; Tfh cells: $CD25^-$, $CXCR3^+CCR6^+$.

Figure 3: UMAP of PBMCs from NU-AS and NU-FRI patients. All cells from (A) NU-AS and (B) NU-FRI coloured by lineage. (C) Volcano plot comparing proportions of 28 metaclusters (MC) between NU-AS and NU-FRI patients. The x-axis shows the difference in means of log2-transformed MC proportions; the y-axis shows the -log10-transformed Benjamini-Hochberg (BH)-adjusted p-value obtained using Welch's t-test. Green points above the horizontal line indicate significantly different clusters. (D) Significantly different clusters and with corresponding cell types and markers. UMAP representation of significantly different clusters in (E) NU-AS and (F) NU-FRI patients. Corresponding heatmaps are provided in Figure S1.

Figure 4: **$CD4^+$ T helper subsets and $CD38^+$ cells in H, NU-AS, and NU-FRI patients.** (A) Tregs, (B) Th1 cells, (C) Th2 cells, (D) Th17 cells, and (E) Tfh cells, (F) $CD38^+$ $CD4^+$ T cells, and (G) $CD38^+$ Tregs in healed (H), NU-AS, and NU-FRI patients. Data shown are from individual patients (H: n=18; NU-AS: n=24; NU-FRI: n=20). Statistical analyses used one-way ANOVA or Kruskal-Wallis tests. Gating strategy: $CD45^+CD66b^-$, $CD19^-CD20^-$, $CD3^+$, $CD4^+$; Tregs: $CCR4^+$, $CD45RA^-CD45RO^+$, $CD127^{low}CD25^{high}$; Th1: $CD25^-$, $CXCR3^+CCR6^-$; Th2: $CD25^-$, $CXCR3^-CCR6^-$; Th17: $CD25^-$, $CXCR3^-CCR6^+$; Tfh: $CD25^-$, $CXCR3^+CCR6^+$.

Figure 5: Monocytes and subsets in H, NU-AS, and NU-FRI patients. (A) Monocytes, (B) classical monocytes, (C) non-classical, and (D) transitional monocytes in healed (H), NU-AS, and NU-FRI patients. Data shown are from individual patients (H: n=18; NU-AS: n=24; NU-FRI: n=20). Statistical analyses used one-way ANOVA or Kruskal-Wallis tests. Gating strategy: Monocytes: $CD45^+CD66b^-$, $CD19^-CD20^-$, $CD3^-CD56^-$, $CD14^+$; classical: $CD38^+$ $CD14^+$; non-classical: $CD14^{low}$, $CD38^-$; transitional: $CD14^+$, $CD38^{low}$.

Figure 6: Receiver operating characteristic curve. (A) ROC curve for the discrimination of NU-AS and NU-FRI based on the number of monocytes and $CD38^+$ Treg cells, as well as their combination; (B) overview of the area under the ROC curve, the optimal cut-off at the maximum Youden index with the corresponding sensitivity and specificity for each biomarker.

Figure 7: Patient recruitment, group assignment, and data. (A) Locations of hospitals participating in the study. (B) NU patients sub-divided into NU-AS and NU-FRI. (C) Summary of clinical data of included patients.

A

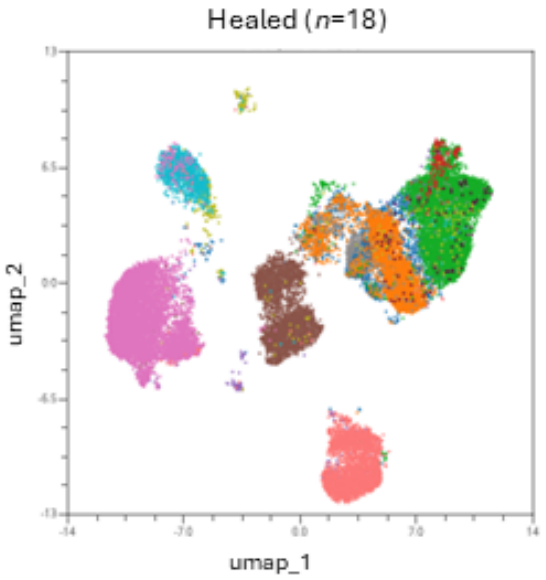

B

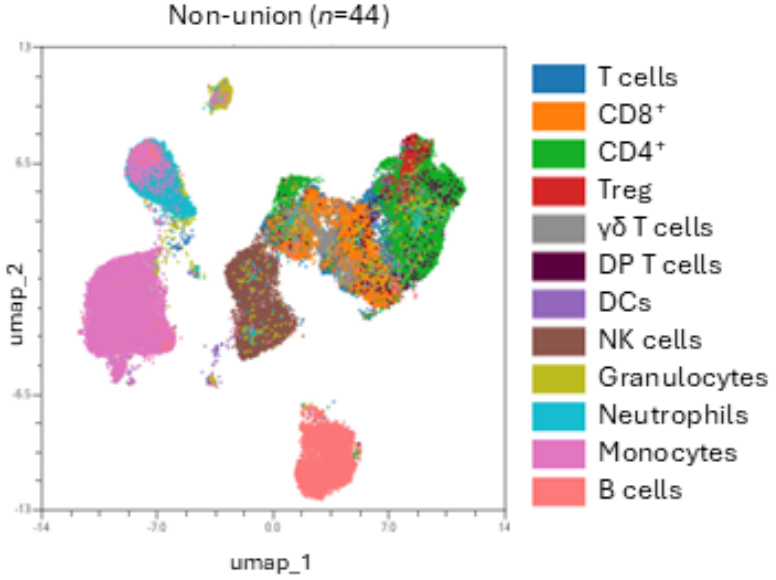

C

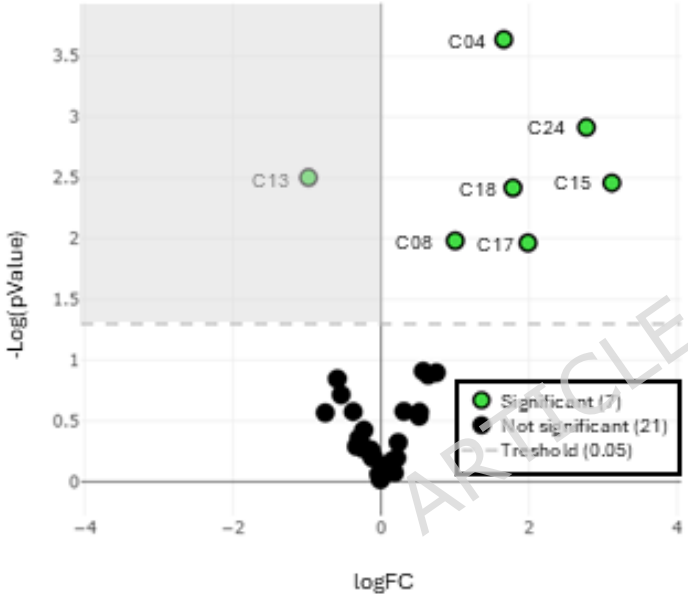

D

Cluster	Cell type	Marker
C04	Granulocytes	CD66b⁺, HLA-DR⁺, CD16⁺, CD11c⁺
C08	CD8⁺ T cells	CD3⁺, CD8⁺
C15	Neutrophils	CD66b⁺, CD16⁺
C17	Granulocytes	CD66b⁺, CD14⁺
C18	CD4⁺ T cells	CD3⁺, CD4⁺
C24	CD4⁺ T cells	CD3⁺, CD4⁺
C13	γδ T cells	CD3⁺, TCRγδ⁺

E

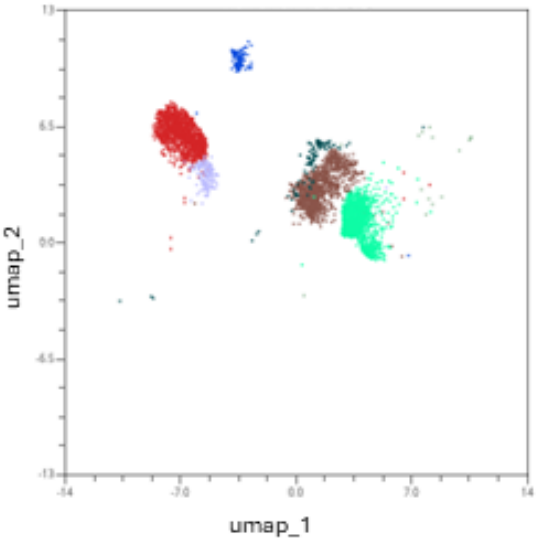

F

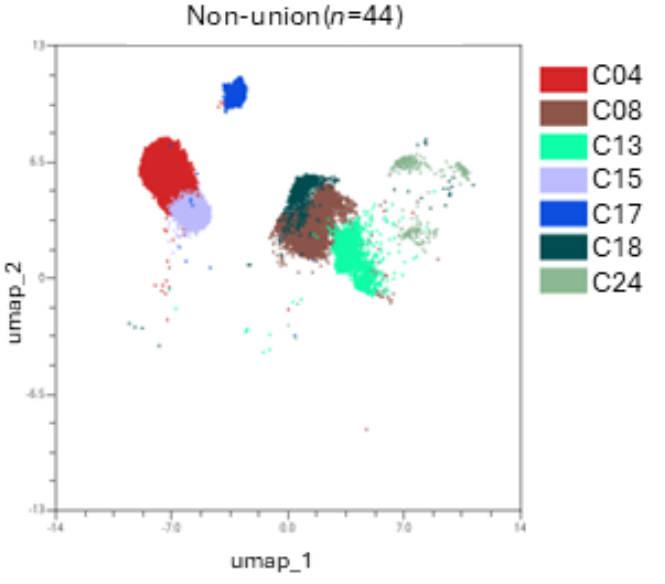

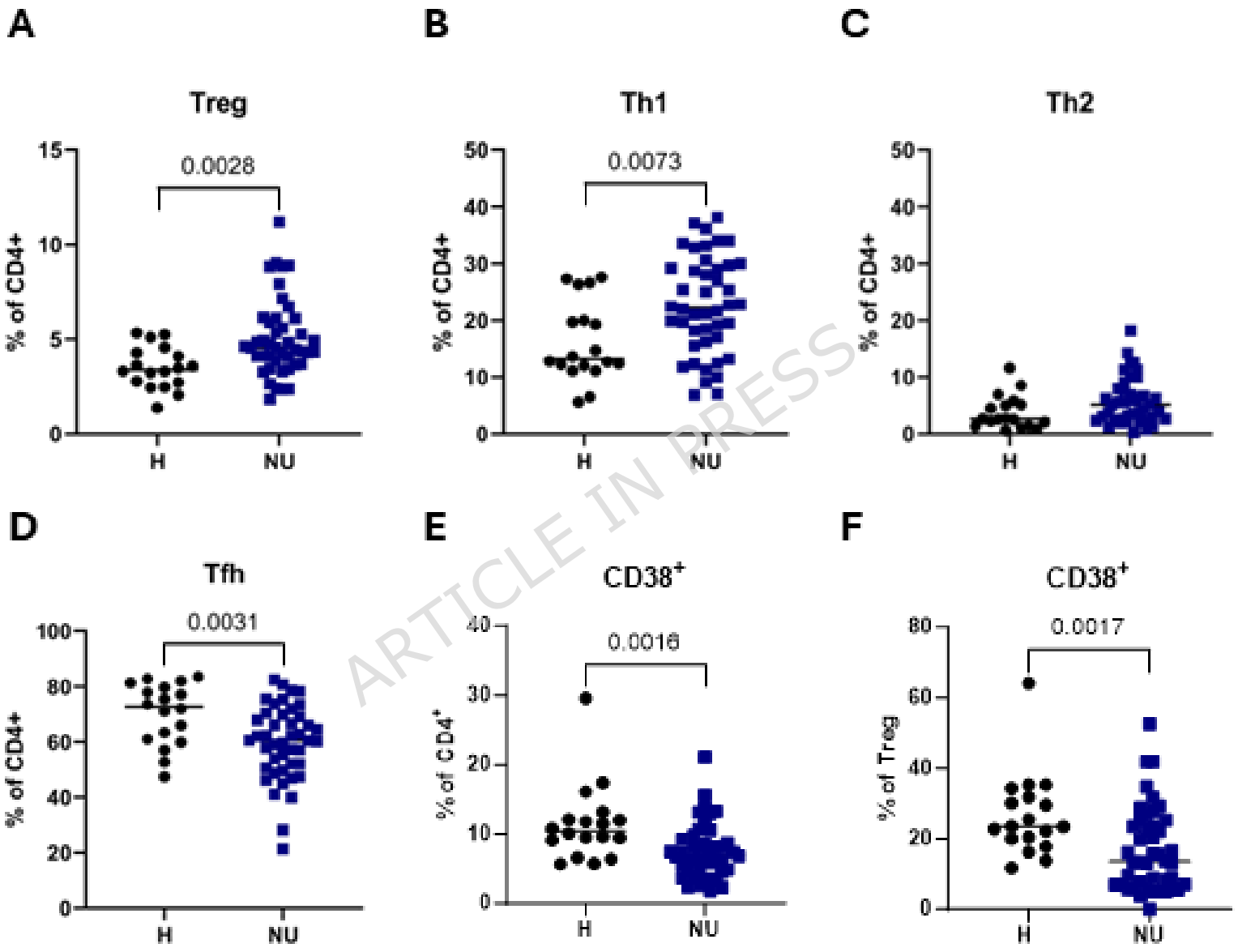

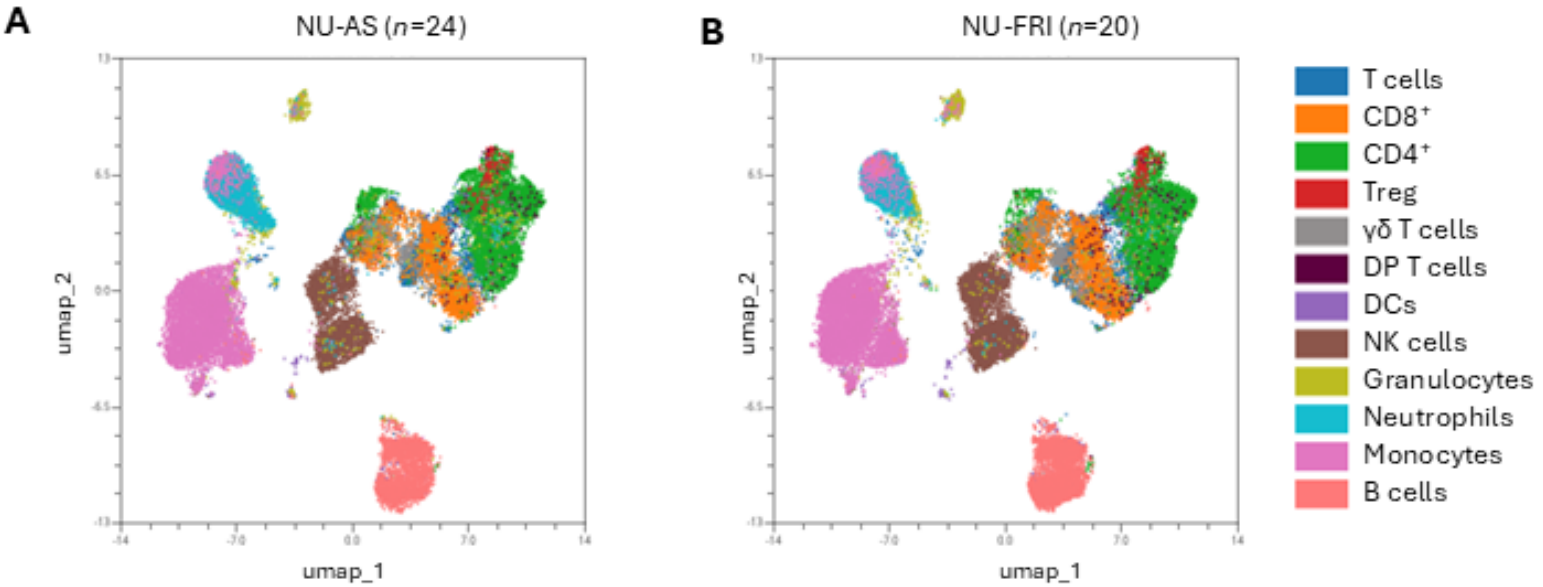

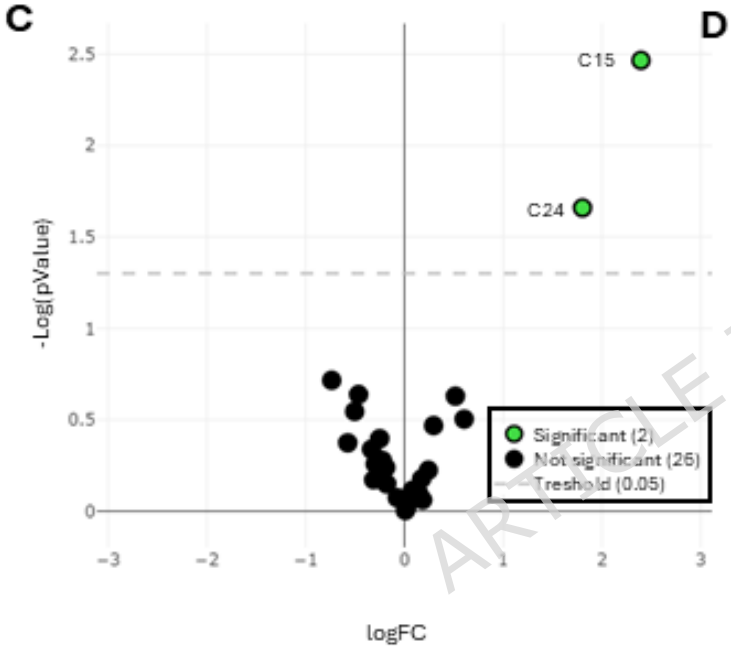

D

Cluster	Cell type	Marker
C15	Neutrophils	CD66b$^+$, CD16$^+$
C24	DP T cells	CD3$^+$, CD4$^+$, CD8$^+$

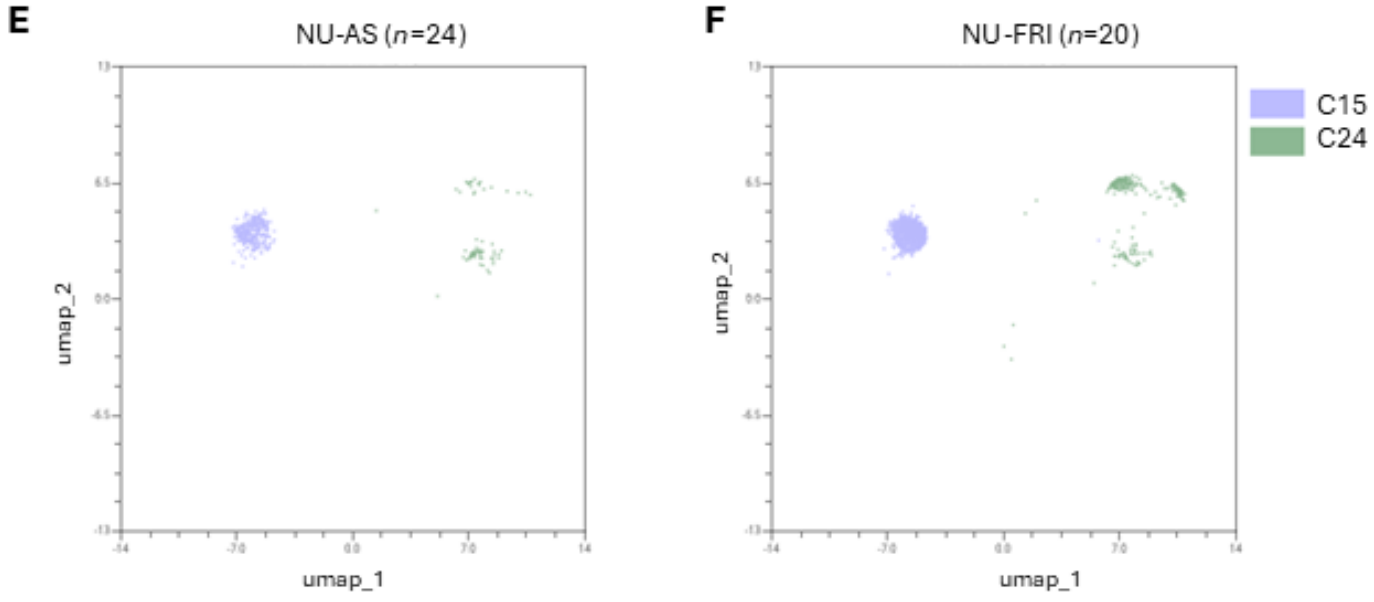

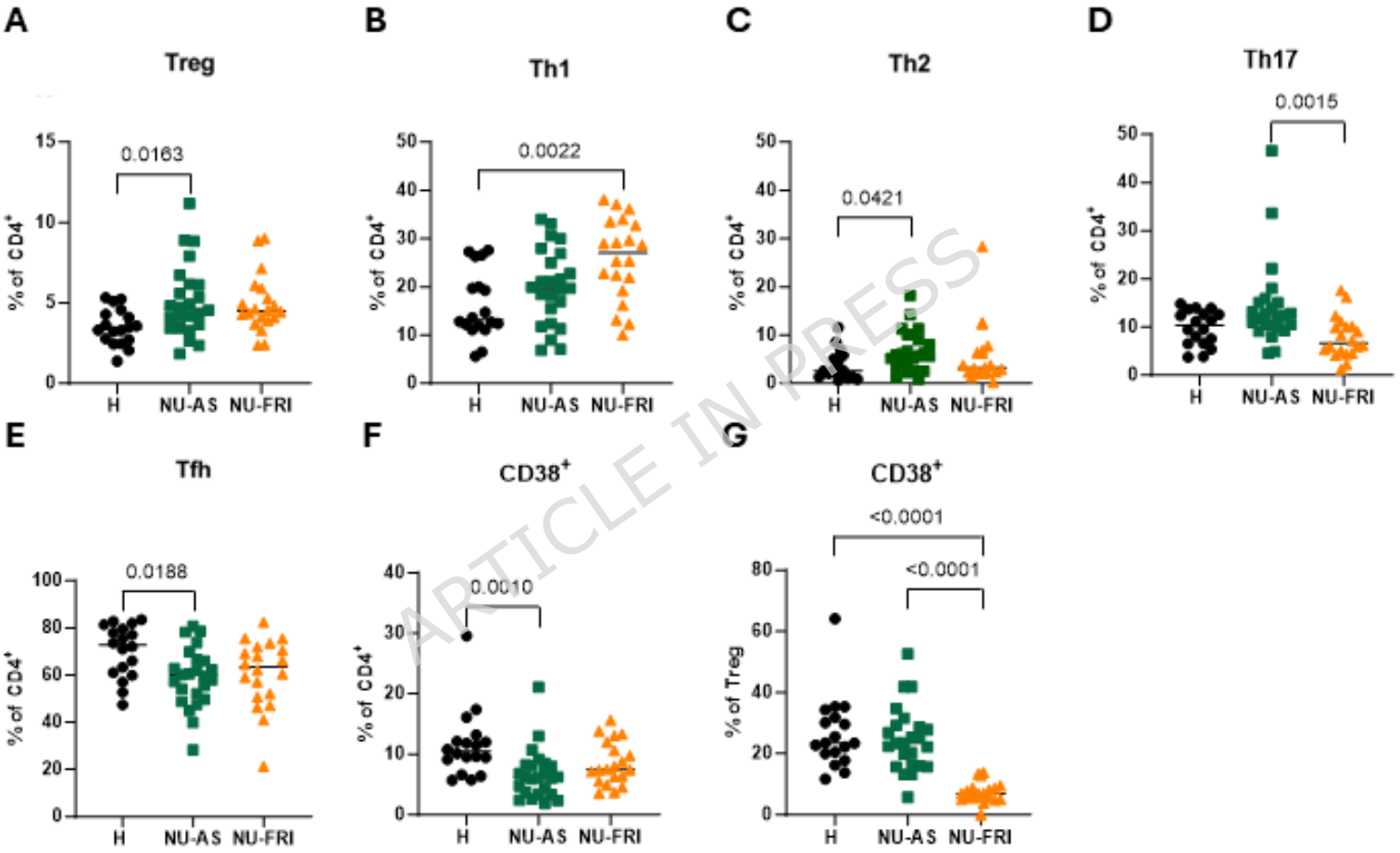

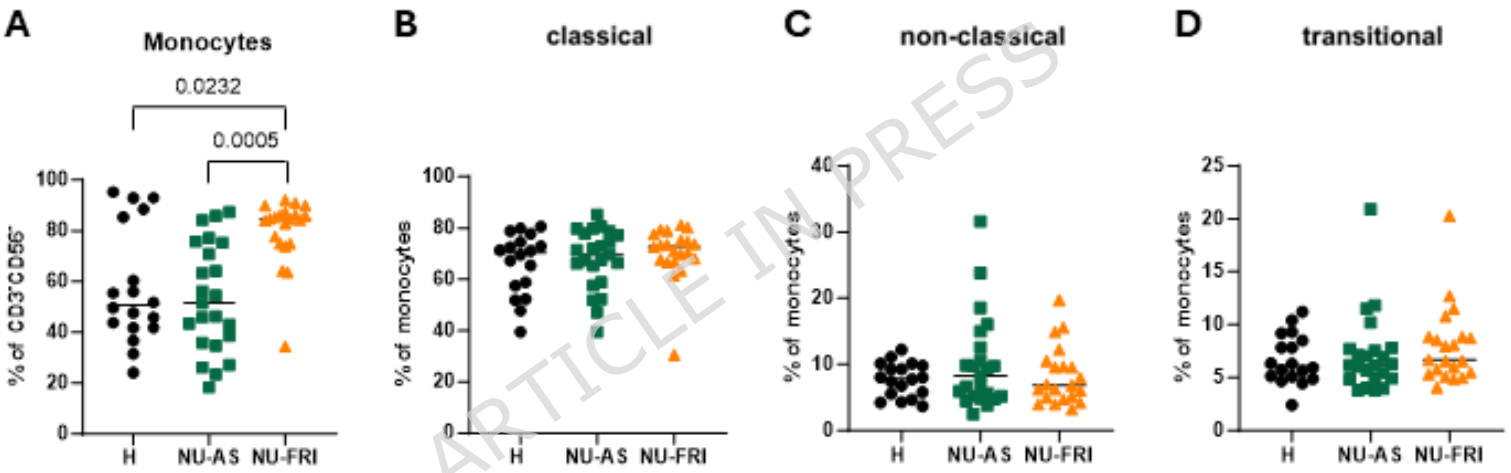

A

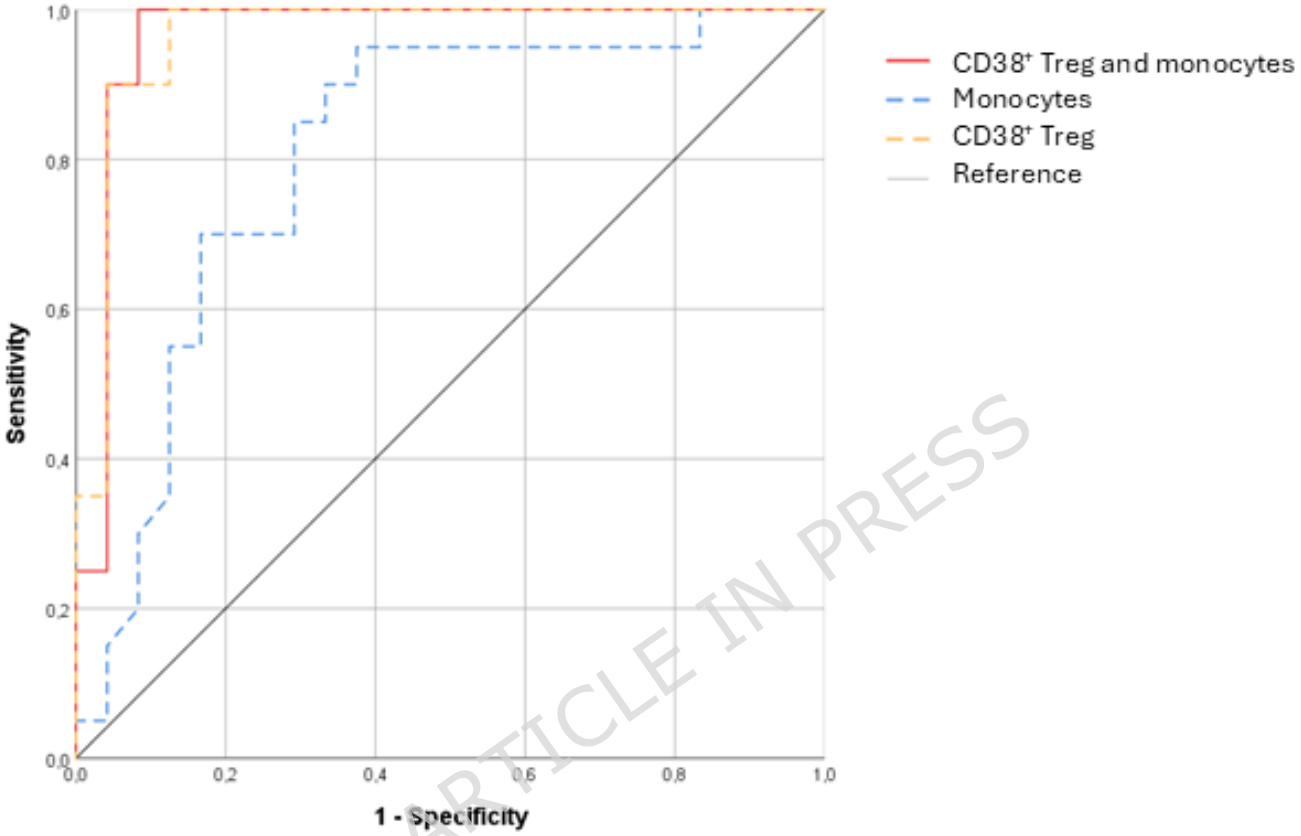

B

Biomarker	AUC (CI)	Youden Index	Cut-off	Sensitivity [%]	Specificity [%]
Monocytes	0.808 (0.675-0.942)	0.58	63.55 % of $CD3^{-}CD56^{-}$	95.0	62.5
$CD38^{+}$ Treg	0.965 (0.909-1.000)	0.88	14.70 % of Treg	100	87.5
$CD38^{+}$ Treg & monocytes	0.965 (0.903-1.000)	0.92	0.34	100	91.7

A

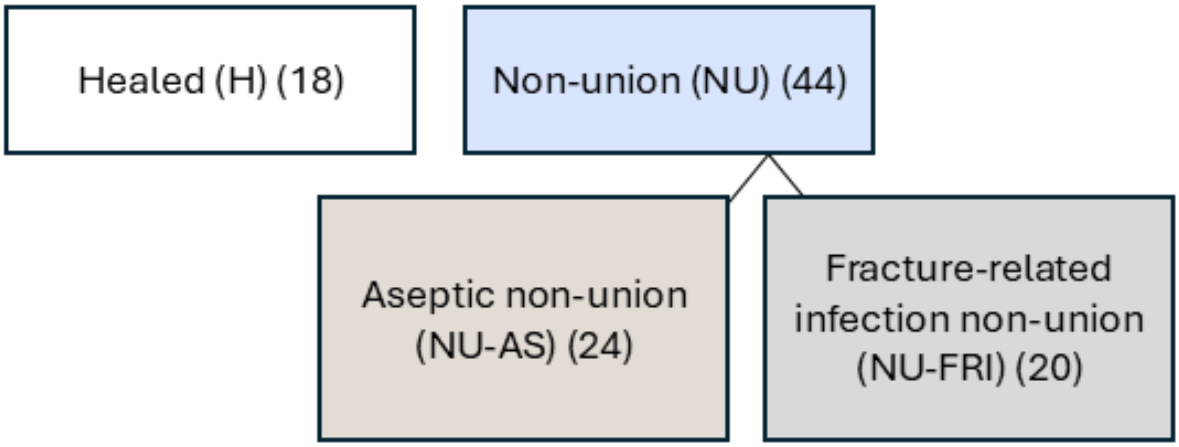

B

Group (number of patients)	H (18)	NU (44)	NU-AS (24)	NU-FRI (20)
% female	27.7%	29.5%	37.5%	25%
Age	41.2±16.2	50.4±17.2	53.6±17.1	46.6±16
BMI	22.9±2.2	28.1±5.7	27.8±5.9	28.3±5.4
Diabetes patients	0%	18%	12.5%	25%
Smoker	22%	9%	12.5%	5%
Polytrauma (no/ yes)	94.4%/ 5.6%	81.8%/ 18.2%	83.3%/ 16.7%	80%/ 20%
Fracture (open/ closed)	16.6%/ 83.4%	52.2%/ 47.8%	17.2%/ 82.2%	50%/ 50%
Bone (Tibia/ Femur)	77.8%/ 22.2%	61.4%/ 38.4%	50%/ 50%	75%/ 25%
Treatment procedure (Plate/ Intramedullary nail)	5.6%/ 94.4%	38.4%/ 61.4%	33.3%/ 66.6%	45%/ 55%
Time between fracture stabilization and non-union revision (days)	-	454.7 (94-1334)	412.5 (162-1254)	505.5 (94-1334)